Selection originating from protein foldability: I. A new method to estimate selection temperature

Sanzo Miyazawa

arXiv:1612.09378v1 [q-bio.PE] 30 Dec 2016

Abstract

The probability distribution of sequences with maximum entropy that satisfies a given amino acid composition at each site and a given pairwise amino acid frequency at each site pair is a Boltzmann distribution with $\exp(-\psi_N)$, where the total interaction ψ_N is represented as the sum of one body and pairwise interactions over all sites and site pairs. A protein folding theory based on the random energy model (REM) indicates that the equilibrium ensemble of natural protein sequences is a canonical ensemble characterized by $\exp(-\Delta G_{ND}/k_BT_s)$ or by $\exp(-G_N/k_BT_s)$ if an amino acid composition is kept constant, where $\Delta G_{ND} \equiv G_N - G_D$, G_N and G_D are the native and denatured free energies, and T_s is the effective temperature of natural selection. Thus, k_BT_s was estimated as the ratio of ΔG_{ND} to $\Delta\psi_{ND}$ or $\Delta\Delta G_{ND}$ to $\Delta\Delta\psi_{ND}$; $\Delta\Delta G_{ND}$ is a folding free energy change due to single amino acid substitutions. Here, we examine interaction changes ($\Delta\psi_N$) due to single nucleotide nonsynonymous mutations, and have found that the variance of their $\Delta\psi_N$ over all sites hardly depends on the ψ_N of each homologous sequence, indicating that the variance of $\Delta G_N (= k_BT_s\Delta\psi_N)$ is nearly constant irrespective of protein families. As a result, T_s is estimated from the ratio of the variance of $\Delta\psi_N$ to that of a reference protein, which is determined by a direct comparison between $\Delta\Delta\psi_{ND} (\simeq \Delta\psi_N)$ and experimental $\Delta\Delta G_{ND}$. Based on the REM, glass transition temperature T_g and ΔG_{ND} are estimated from T_s and experimental melting temperatures (T_m) for 14 protein domains. The estimates of ΔG_{ND} agree well with their experimental values for 5 proteins, and those of T_s and T_g are all within a reasonable range. This method is coarse-grained but much simpler in estimating T_s, T_g and $\Delta\Delta G_{ND}$ than previous methods.

Insert Received for publication Date and in final form Date.

sanzo.miyazawa@gmail.com

© 2013 The Authors
0006-3495/08/09/2624/12 $2.00 doi: 10.1529/biophysj.106.090944

Natural proteins can fold their sequences into unique structures. Protein's stability and foldability result from natural selection and are not typical characteristics of random polymers (1–3). Natural selection maintains protein's stability and foldability over evolutionary timescales. On the basis of the random energy model (REM) for protein folding, Pande et al. (3) discussed that the equilibrium ensemble of natural protein sequences is a canonical ensemble characterized by a Boltzmann factor $\exp(-\Delta G_{ND}(\boldsymbol{\sigma})/k_BT_s)$, where $\Delta G_{ND}(\boldsymbol{\sigma})(\equiv G_N(\boldsymbol{\sigma}) - G_D(\boldsymbol{\sigma}))$ is the folding free energy of sequence $\boldsymbol{\sigma}$, G_N and G_D are the free energies of the native and denatured states, k_B is the Boltzmann constant, and T_s is the effective temperature of natural selection and must satisfy $T_s < T_g < T_m$ for natural proteins to fold into unique native structures; T_g is glass transition temperature and T_m is melting temperature; see subsection 4.1 for details. The REM also indicates that the free energy of denatured conformations (G_D) is a function of amino acid frequencies only and does not depend on amino acid order, and therefore the Boltzmann factor will be taken as $\exp(-G_N(\boldsymbol{\sigma})/k_BT_s)$, if amino acid frequencies are kept constant.

On the other hand, the maximum entropy principle insists that the probability distribution of sequences in sequence space, which satisfies constraints on amino acid compositions at all sites and on amino acid pairwise frequencies for all site pairs, is a Boltzmann distribution with the Boltzmann factor $\exp(-\psi_N(\boldsymbol{\sigma}))$, where $\psi_N(\boldsymbol{\sigma})$ is the total interaction of a native sequence $\boldsymbol{\sigma}$ and represented as the sum of one-body (h) and pairwise (J) interactions between residues in the sequence; see subsection 4.2 for details. The one-body (h) and pairwise (J) residue-residue interactions that satisfy those constraints for homologous sequences have been estimated (4–7) as one of Potts problems and successfully used to predict contacting residue pairs in protein structures (4–10).

Morcos et al. (11) noticed that the ψ_N in the Boltzmann factor is the dimensionless energy corresponding to G_N/k_BT_s, and estimated effective temperatures (T_s) of natural selection for several protein families by comparing the difference ($\Delta\psi_{ND}$) of ψ between the native and the molten globule states with folding free energies (ΔG_{ND}) estimated with associativememory, water-mediated, structure, and energy model (AWSEM) (12).

Here, we estimate the effective temperature of natural selection (T_s) and then glass transition temperature (T_g) and folding free energy (ΔG_{ND}) of protein from the effects ($\Delta\psi_N$) of single amino acid substitutions on the total interaction of a protein in the equilibrium ensemble of sequences. We estimate the one-body (h) and pairwise (J) interactions with the DCA program, which is available at "http://dca.rice.edu/portal/dca/home", and then examine the changes ($\Delta\psi_N$) of the total interaction (ψ_N) of a native sequence due to single amino acid substitutions caused by single nucleotide changes. The data of $\Delta\psi_N$ due to single nucleotide nonsynonymous substitutions for 14 protein families show that the variance of $\Delta\psi_N$ over all the substitutions at all sites hardly depends on the total interaction (ψ_N) of each homologous sequence and is nearly constant for each protein family, indicating that the variance of $\Delta G_N(= k_BT_s\Delta\psi_N)$ is nearly constant irrespective of protein families. From this finding, T_s for each protein family has been estimated in relative to T_s for the PDZ family, which is determined by directly comparing $\Delta\Delta\psi_{ND}(\simeq \Delta\psi_N)$ with experimental $\Delta\Delta G_{ND}$. Also, T_g and the ΔG_{ND} for each protein family are estimated on the basis of the REM from the estimated T_s and an experimental melting temperature T_m. The estimates of ΔG_{ND} are well compared with experimental ΔG_{ND} for 5 protein families. The present method for estimating T_s is simpler than the method (11) using AWSEM, and also is useful for the prediction of ΔG_{ND}, because the experimental data of ΔG_{ND} are limited in comparison with T_m, and also experimental conditions such as temperature and pH tend to be different among them. In addition, it has been revealed that $\Delta\psi_N$ averaged over all single nucleotide nonsynonymous substitutions is a linear function of ψ_N/L of each homologous sequence, where L is a sequence length; the average of $\Delta\psi_N$ decreases as ψ_N/L increases. As shown in the succeeding manuscript (13), this characteristic is required for homologous proteins to stay at the equilibrium state of the native conformational energy $G_N = k_BT_s\psi_N$, and indicates a weak dependency of $\Delta\Delta G_{ND}$ on $\Delta G_{ND}/L$ of protein across protein families.

1 Materials

1.1 Sequence data

We study the single domains of 8 Pfam (14) families and both the single domains and multi-domains from 3 Pfam families. In Table 1, their Pfam ID for a multiple sequence alignment, and Uniprot ID and PDB ID with the starting- and ending-residue positions of the domains are listed. The full alignments for their families at the Pfam are used to estimate one-body interactions h and pairwise interactions J with the DCA program from "http://dca.rice.edu/portal/dca/home" (4, 5). To estimate the sample ($\overline{\psi_N}$) and ensemble ($\langle\psi_N\rangle_{\boldsymbol{\sigma}}$) averages of the total interaction, M unique sequences with no deletion are used. In order to reduce phylogenetic biases in the set of homologous sequences, we employ a sample weight ($w_{\boldsymbol{\sigma}_N}$) for each sequence, which is equal to the inverse of the number of sequences that are less than 20% different from a given sequence in a given set of homologous sequences. Only representatives of unique sequences with no deletion, which are at least 20% different from each other, are used to calculate the changes of the total interaction ($\Delta\psi_N$) due to single nucleotide nonsynonymous substitutions; the number of the representatives is almost equal to $M_{\rm eff}$ in Table 1.

2 Results

2.1 Important parameters in the estimations of one-body and pairwise interactions, h and J, and of the total interaction, $\psi_N(\boldsymbol{\sigma})$

There are two methods available to estimate one-body (h) and pairwise (J) interactions for amino acid order in a protein sequence; $\psi_N(\boldsymbol{\sigma}) = -(\sum_i h_i(\sigma_i) + \sum_{j>i} J_{ij}(\sigma_i, \sigma_j))$, where $\boldsymbol{\sigma} \equiv (\sigma_1, \cdots, \sigma_L)$ and $\sigma_i \in$ {amino acids, deletion}. See the Supporting Material for details. One of them is a method called the pseudo-likelihood maximization (plmDCA) method (6, 7) in which a pseudo-likelihood with a l_2 regularization term is maximized. Another method is the DCA method (4, 5) in which pairwise (J) interactions are estimated in the mean-filed approximation for a Potts problem.

In the plmDCA, a l_2 regularization term is equal to $\lambda_h \|\boldsymbol{h}\| + \lambda_J \|\boldsymbol{J}\|$, which is a weighted sum of the vector and matrix norms of h and J. The λ_h and λ_J are a parameter and the optimum values of $\|\boldsymbol{h}\|$ and $\|\boldsymbol{J}\|$ depend strongly on their values. In the case of $\lambda_h = \lambda_J = 0.01$, which seem to be appropriate for contact predictions (6, 7), the values of $\|\boldsymbol{h}\|$ and $\|\boldsymbol{J}\|$ are too small to yield reasonable values for an effective temperature (T_s) of selection. To get an appropriate range of values for $\|\boldsymbol{h}\|$ and $\|\boldsymbol{J}\|$, even $\lambda = 0.0001$ may be too large. Thus, we use the DCA here rather than the plmDCA, although the plmDCA was very successful in contact predictions. In the case of the DCA method, the ratio of pseudocount ($0 \le p_c \le 1$) defined in Eqs. S51 and S52 is a parameter and controls the values of the ensemble and sample averages of ψ_N in sequence space, $\langle \psi_N(\boldsymbol{\sigma}) \rangle_{\boldsymbol{\sigma}}$ in Eq. A25 and $\overline{\psi_N(\boldsymbol{\sigma}_N)}$ in Eq. A28; a weight for observed counts is defined to be equal to $(1 - p_c)$. Sample average means the average over all homologous sequences with a weight for each sequence to reduce phylogenetic biases. An appropriate value must be chosen for the ratio of pseudocount in a reasonable manner.

Another problem is that the estimates of h and J (4, 5) include a lot of noise as a result of estimating too many interaction parameters from a relatively small number of sequences, and J_{ij} may take significant values even for site pairs that are distantly located in the three dimensional structure of protein. Therefore, according to Morcos et al. (11), the estimate of J is modified as follows.

$$\hat{J}_{ij}(a_k, a_l) \quad = \quad J^{\mathrm{g}}_{ij}(a_k, a_l) H(r_{\mathrm{cutoff}} - r_{ij}) \tag{1}$$

where J^{g} is the statistical estimate of J in a certain gauge, $a_k \in$ {amino acids, deletion}, H is the Heaviside step function, and r_{ij} is the distance between the centers of amino acid side chains at sites i and j in a protein structure, and r_{cutoff} is a distance threshold for residue pairwise interactions. If pairwise interactions are cut off at a certain distance, the estimate of the total interaction will depend on the choice of gauge for h and J; see the Method section in the Supplement for details. The sample and ensemble averages of the total interactions per residue over homologous sequences in the PDZ domain family are plotted against the cutoff distance in Fig. S1 in the Supporting Material. The solid and dotted lines indicate the sample and ensemble averages, respectively, and the plus (black) and cross (blue) marks show those for the simple and Ising gauges, respectively. In the simple gauge, $\sum_k h^s_i(a_k) = \sum_{k,l} J^s_{ij}(a_k, a_l) = 0$; see Eqs. S56 and S57. On the other hand, one-body interaction (h^I) in the Ising gauge is generated (7) from any gauge by $h^{\mathrm{I}}_i(a_k) = h^{\mathrm{g}}_i(a_k) - h^{\mathrm{g}}_i(:) + \sum_{j \ne i}(J^{\mathrm{g}}_{ij}(a_k, :) - J^{\mathrm{g}}_{ij}(:, :))$; see Eqs. S44 and S45. Those for the simple and Ising gauges agree with each other at a sufficiently large value of the cutoff where all pairwise interactions are included. If pairwise interactions are cut off at a certain distance, however, they will yield very different values for the total interaction. Here the simple gauge is employed, because in the Ising gauge the one-body interactions (h^{I}_i) include interactions originated in pairwise interactions (J^{g}_{ij}) beyond the cutoff distance; see Eq. S45.

Candidates for the cutoff distance may be about 8 Å for the first interaction shell and 15-16 Å for the second interaction shell between residues; distance between the centers of side chain atoms is employed for residue distance. Here both the distances are tested for the cutoff distance. An appropriate value for the ratio of pseudocount for the certain cutoff distance, either about 8 Å or 15-16 Å , is chosen for each protein family in such a way that the sample average of the total interactions must be equal to the ensemble average, $\overline{\psi_N} = \langle \psi_N \rangle_{\boldsymbol{\sigma}}$; see Eqs. A25 and A29. In the present multiple sequence alignment for the PDZ domain, with the ratios of pseudocount $p_c = 0.205$ and $p_c = 0.33$, the sample and ensemble averages agree with each other at the cutoff distances $r_{\mathrm{cutoff}} \sim 8$ Å and $r_{\mathrm{cutoff}} \sim 15.5$ Å , respectively; see Fig. S1. In Fig. S2, the reflective correlation and regression coefficients between the experimental $\Delta\Delta G_{ND}$ (15) and $\Delta\psi_N$ due to single amino acid substitutions are plotted against the cutoff distance for pairwise interactions in the PDZ domain. The reflective correlation has the maximum at the $r_{\mathrm{cutoff}} \sim 8$ Å for $p_c = 0.205$ and at $r_{\mathrm{cutoff}} \sim 15.5$ Å for $p_c = 0.33$, indicating that these cutoff distances are appropriate for those ratios of pseudocount. The ratio of pseudocount and a cutoff distance employed are listed for each protein family in Tables 2 and S5 for $r_{\mathrm{cutoff}} \sim 8$ and 15.5Å , respectively.

2.2 Changes of the total interaction, $\Delta\psi_N$, by single nucleotide nonsynonymous substitutions

The change of the total interaction of a native conformation by a single amino acid substitution from σ_i^N to σ_i at site i in a native sequence $\boldsymbol{\sigma}_N$ is defined as

$$\begin{aligned}
\Delta\psi_N(\sigma_{j\neq i}^N, \sigma_i^N \to \sigma_i) &\equiv \psi_N(\sigma_{j\neq i}^N, \sigma_i) - \psi_N(\boldsymbol{\sigma}_N) && (2)\\
\Delta\psi_D(\sigma_{j\neq i}^N, \sigma_i^N \to \sigma_i, T) &\equiv \psi_D(\sigma_{j\neq i}^N, \sigma_i, T) - \psi_D(\boldsymbol{\sigma}_N, T) && (3)\\
\Delta\Delta\psi_{ND}(\sigma_{j\neq i}^N, \sigma_i^N \to \sigma_i) &\equiv \Delta\psi_N(\sigma_{j\neq i}^N, \sigma_i^N \to \sigma_i) - \Delta\psi_D(\sigma_{j\neq i}^N, \sigma_i^N \to \sigma_i) && (4)\\
&\simeq \Delta\psi_N(\sigma_{j\neq i}^N, \sigma_i^N \to \sigma_i) \quad \text{because } \boldsymbol{f}(\boldsymbol{\sigma}_N) \approx \boldsymbol{f}(\sigma_{j\neq i}^N, \sigma_i) && (5)
\end{aligned}$$

Here, single amino acid substitutions caused by single nucleotide nonsynonymous mutations are taken into account, unless specified. Let us use a single overline to denote the average of the changes of interaction over all types of single nucleotide nonsynonymous mutations at all sites in a specific native sequence, and a double overline to denote their averages over all homologous sequences in a protein family.

We calculated the ψ_N of native amino acid sequences and $\Delta\psi_N$ due to all types of single nucleotide nonsynonymous substitutions for all homologous sequences, and their means and variances. We has examined the dependence of $\overline{\Delta\Delta\psi_{ND}} \simeq \overline{\Delta\psi_N}$ on the ψ_N of each homologous sequence in each protein family. Fig. 1 for the PDZ family shows that $\overline{\Delta\psi_N}$ is negatively proportional to the ψ_N/L of the wildtype, that is,

$$\begin{aligned}
&\overline{\Delta\Delta\psi_{ND}(\sigma_{j\neq i}^N, \sigma_i^N \to \sigma_i)} \simeq \overline{\Delta\psi_N(\sigma_{j\neq i}^N, \sigma_i^N \to \sigma_i)}\\
&\quad\approx\quad \alpha_{\psi_N}\frac{\psi_N(\boldsymbol{\sigma}_N) - \overline{\psi_N(\boldsymbol{\sigma}_N)}}{L} + \overline{\overline{\Delta\psi_N(\sigma_{j\neq i}^N, \sigma_i^N \to \sigma_i)}} \qquad \text{with } \alpha_{\psi_N} < 0 \qquad (6)
\end{aligned}$$

where L is sequence length. This relationship is found in all of the protein families examined here; the correlation and regression coefficients for $r_{\text{cutoff}} \sim 8$ and 15.5Å are listed in Tables 2 and S5, respectively. Most of the correlation coefficients are larger than 0.95, and all are greater than 0.9. It is reasonable that the change of the total interaction ($\Delta\psi_N$) depends on interaction per residue (ψ_N/L) rather than the total interaction (ψ_N), because interactions change only for one residue substituted in the sequence. On this line of consideration, the following approximation for the slope is confirmed in Fig. S8.

$$\alpha_{\psi_N} \approx \overline{\overline{\Delta\psi_N(\sigma_{j\neq i}^N, \sigma_i^N \to \sigma_i)}}/(-\delta\psi^2/L) \qquad (7)$$

The important fact is that the linear dependence of $\Delta\psi_N$ on ψ_N/L shown in Fig. 1 and Tables 2 and S5 is equivalent to the linear dependence of free energy changes caused by single amino acid substitutions on the native conformational energy of the wildtype protein, because the selection temperatures T_S of homologous sequences in a protein family are approximated to be equal.

Is the same type of dependence on ψ_N/L found for the standard deviation of $\Delta\psi_N$ over single nucleotide nonsynonymous substitutions at all sites? Fig. 1 and Tables 2 and S5 show that the correlation between the standard deviation of $\Delta\psi_N$ and ψ_N of the wildtype is very weak except for Nitroreductase, SBP_bac_3 and LysR_substrate families. Even for these protein families, the regression coefficients are less negative than those for $\overline{\Delta\psi_N}$. Thus, it is indicated that in general the variance/standard deviation of $\Delta\psi_N$ due to single amino acid substitutions is almost constant irrespectively of the ψ_N across homologous sequences.

2.3 Effective temperature T_s of selection estimated from the changes of interaction, $\Delta\psi_N$, by single nucleotide nonsynonymous substitutions

The variance of $\Delta\psi_N$ must be approximated by a function of k_BT_s, because it does not depend on ψ_N of the wildtype and is nearly constant across homologous sequences in every protein family that has its own characteristic temperature (Ts) for natural selection. On the other hand, the free energy of the native structure, ΔG_N, may be approximated by a function of G_N but must not explicitly depend on k_BT_s. In other words, the following relationships are derived.

$$\begin{aligned}
\text{Var}(\Delta\psi_N(\sigma_{j\neq i}^N, \sigma_i^N \to \sigma_i)) &\approx \text{independent of } \psi_N \text{ and}\\
&\quad \text{constant across homologous sequences in every protein family} && (8)\\
&= \text{function of } k_BT_s && (9)\\
\text{Var}(\Delta G_N(\sigma_{j\neq i}^N, \sigma_i^N \to \sigma_i)) &= \text{function that must not explicitly depend on } k_BT_s \text{ but } G_N && (10)
\end{aligned}$$

From the equations above, we obtain the important relation that the variance of $\Delta G_N(= k_B T_s \Delta\psi_N)$ does not depend on G_N and is nearly constant irrespective of protein families.

$$\begin{aligned} \mathrm{Var}(\Delta G_N(\sigma^N_{j\neq i}, \sigma^N_i \rightarrow \sigma_i)) &= (k_B T_s)^2 \,\mathrm{Var}(\Delta\psi_N(\sigma^N_{j\neq i}, \sigma^N_i \rightarrow \sigma_i)) \\ &\approx \text{constant} \end{aligned} \tag{11}$$

This relationship is consistent with the observation that the variance of $\Delta\Delta G_{ND}(\simeq \Delta G_N)$ is nearly constant irrespectively of protein families ($\Delta G_{ND}(\simeq G_N)$) (16). This relationship allows us to estimate a selection temperature (T_s) for a protein family in a scale relative to that of a reference protein from the ratio of the standard deviation of $\Delta\psi_N$. The PDZ family is employed here as a reference protein, and its T_s is estimated by a direct comparison of $\Delta\psi_N$ and experimental $\Delta\Delta G_{ND}$; because the experimental data of $\Delta\Delta G_{ND}$ are available for many types of single amino acid substitutions in the PDZ domain.

$$k_B\hat{T}_s = k_B\hat{T}_{s,\,\mathrm{PDZ}}\,[\,\overline{\mathrm{Var}(\Delta\psi_{\mathrm{PDZ}}(\sigma^N_{j\neq i}, \sigma^N_i \rightarrow \sigma_i))}\,/\,\overline{\mathrm{Var}(\Delta\psi_N(\sigma^N_{j\neq i}, \sigma^N_i \rightarrow \sigma_i))}\,]^{1/2} \tag{12}$$

where the overline denotes the average over all homologous sequences. Here, the averages of variances over all homologous sequences are employed, because T_s for all homologous sequences are approximated to be equal.

2.4 A direct Comparison of the changes of interaction, $\Delta\psi_N(\simeq \Delta\Delta\psi_{ND})$, with the experimental $\Delta\Delta G_{ND}$ due to single amino acid substitutions

The effective temperature (T_s) of selection for the PDZ family has bee estimated by directly comparing $\Delta\psi_N(\simeq \Delta\Delta\psi_{ND})$ with experimental $\Delta\Delta G_{ND}$ (15) for single amino acid substitutions. In Fig. 2 the experimental values (15) of $\Delta\Delta G_{ND}$ due to single amino acid substitutions in the PDZ domain are plotted against the changes of interaction, $\Delta\psi_N$ for the same types of substitutions. The slopes of the least-squares regression lines through the origin, which are estimates of $k_B T_s$, are equal to $k_B\hat{T}_s = 0.279$ kcal/mol for $r_{\mathrm{cutoff}} \sim 8$ Å and $k_B\hat{T}_s = 0.162$ kcal/mol for $r_{\mathrm{cutoff}} \sim 15.5$ Å , and the reflective correlation coefficients are equal to 0.93 and 0.94, respectively.

These estimates of $k_B T_s$, 0.279 and 0.162, for the PDZ yield $(\overline{\mathrm{Var}(\Delta\Delta G_{ND})})^{1/2} = 1.28$ kcal/mol, which corresponds to 75% of 1.7 kcal/mol (17) estimated from ProTherm database or 79% of 1.63 kcal/mol (16) computationally predicted for single nucleotide mutations by using the FoldX. Using $(\overline{\mathrm{Var}(\Delta\Delta G_{ND})})^{1/2} = 1.28$kcal/mol estimated from T_s for PDZ, the absolute values of T_s for other proteins are calculated by Eq. 12 and listed in Table 3 and S6. Fig. 3 shows that $r_{\mathrm{cutoff}} \sim 15.5$ Å yields slightly larger values in a scale relative to the T_s of the PDZ but lower absolute values of T_s for all the proteins than $r_{\mathrm{cutoff}} \sim 8$ Å.

Morcos et al. (11) estimated T_s by comparing $\Delta\psi_{ND}$ with ΔG_{ND} estimated by the associativememory, water-mediated, structure, and energy model (AWSEM). They estimated ψ_N with $r_{\mathrm{cutoff}} = 16$ Å and probably $p_c = 0.5$; the gauge employed is unknown. In Fig. S7, the present estimates of T_s are compared with those by Morcos et al. (11).

2.5 Expected dependency of folding free energy change ($\Delta\Delta G_{ND}$) due to single nucleotide nonsynonymous substitutions on folding free energy per residue ($\Delta G_{ND}/L$)

Let us consider the average of $\overline{\Delta\psi_N}$ over homologous sequences in each protein family. The following regression line is shown in Fig. 4.

$$\overline{\overline{\Delta\psi_N(\sigma^N_{j\neq i}, \sigma^N_i \rightarrow \sigma_i)}} \approx \alpha_{\overline{\psi_N}} \frac{\overline{\psi_N(\boldsymbol{\sigma}_N)} - \bar{\psi}(\overline{\boldsymbol{f}(\boldsymbol{\sigma}_N)})}{L} + \beta_{\overline{\psi_N}} \tag{13}$$

$$= \alpha_{\overline{\psi_N}} \frac{-\delta\psi^2(\overline{\boldsymbol{f}(\boldsymbol{\sigma}_N)})}{L} + \beta_{\overline{\psi_N}} \tag{14}$$

$$\alpha_{\overline{\psi_N}} < 0 \quad , \quad \beta_{\overline{\psi_N}} \approx 0 \tag{15}$$

Here, $\overline{\psi_N(\boldsymbol{\sigma}_N)}$ is reduced by $\bar{\psi}$ because the origin of the ψ_N scale is not unique. The correlation between $\overline{\overline{\Delta\psi_N}}$ and $\delta\psi^2/L$ is significant; the correlation coefficient is larger than 0.99. It should be noted here that the intercept $\beta_{\overline{\psi_N}}$ should be equal to 0, because if $T_s \rightarrow \infty$ then $\delta\psi^2 \rightarrow 0$ and $\Delta\psi_N \rightarrow 0$. Actually, Fig. 4 shows that $\beta_{\overline{\psi_N}}$ is nearly equal to 0.

Finally, the dependence of $\Delta\Delta G_{ND}$ on ΔG_{ND} can be predicted.

$$\overline{\overline{\Delta\Delta G_{ND}(\sigma^N_{j\neq i}, \sigma^N_i \to \sigma_i)}} \approx -\alpha_{\delta\psi^2} k_B T_s \frac{\delta\psi^2(\overline{\boldsymbol{f}(\boldsymbol{\sigma}_N)})}{L} + \beta_{\delta\psi^2} \quad (16)$$

$$\approx \alpha_{\Delta G_{ND}} k_B T_s \frac{\delta\psi^2(\overline{\boldsymbol{f}(\boldsymbol{\sigma}_N)})}{L} (\vartheta(T/T_g)\frac{T_s}{T} - 1) + \beta_{\Delta G_{ND}} \quad (17)$$

$$= \alpha_{\Delta G_{ND}} \frac{\langle \Delta G_{ND}(\boldsymbol{\sigma}_N, T)\rangle}{L} + \beta_{\Delta G_{ND}} \quad (18)$$

In general, T_s and T_g are different among protein families, so that the correlation between $\overline{\overline{\Delta\Delta G_{ND}}}$ and $\langle \Delta G_{ND}\rangle/L$ cannot be strong. In Fig. 5, $\overline{\overline{\Delta\Delta G_{ND}}}$ for the present proteins are plotted against $\langle \Delta G_{ND}\rangle/L$. However, it should be noted that the correlation is not expected for $\overline{\overline{\Delta\Delta G_{ND}}}$ and $\langle \Delta G_{ND}\rangle$ but for $\overline{\overline{\Delta\Delta G_{ND}}}$ and $\langle \Delta G_{ND}\rangle/L$.

2.6 Estimation of T_g, ω, and $\langle \Delta G_{ND}(\boldsymbol{\sigma})\rangle_{\boldsymbol{\sigma}}$ from T_s and T_m

To estimate glass transition temperature T_g, the conformational entropy per residue ω in the compact denatured state, and the ensemble average of folding free energy in sequence space $\langle \Delta G_{ND}\rangle_{\boldsymbol{\sigma}}$, melting temperature T_m must be known for each protein; see Eqs. A30, A18, and A27 for T_g, ω and $\langle \Delta G_{ND}\rangle_{\boldsymbol{\sigma}}$, respectively. The experimental value of T_m employed for each protein is listed in Table 3 and S6. For comparison, temperature T is set up to be equal to the experimental temperature for ΔG_{ND} or to 298°K if unknown.

An estimate of glass transition temperature, $\hat{T}_g$, has been calculated with $\hat{T}_s$ and T_m by Eq. A30, and is listed in Table 3 and S6 for each protein. In Fig. 6, $\hat{T}_s/\hat{T}_g$ is plotted against $T_m/\hat{T}_g$ for each protein family. Unless $T_g < T_m$, a protein will be trapped at local minima on a rugged free energy landscape before it folds into a unique native structure. Protein foldability increases as T_m/T_g increases. A condition, $\Delta G_{ND} = 0$ at $T = T_m$, for the first order transition requires that Eq. A30, which is indicated by a dotted curve in Fig. 6, must be satisfied. As a result, T_s/T_g must be lowered to increase T_m/T_g; in other words, proteins must be selected at lower T_s. The present estimates of T_s and T_g would be within a reasonable range (11, 18, 19) of values required for protein foldability.

In Table 3 and S6, the ensemble average of $\Delta G_{ND}(\boldsymbol{\sigma})$ over sequences calculated by Eq. A27, and the conformational entropy per residue ω in the compact denatured state by Eq. A18 are also listed for each protein. Fig. 7 shows the comparison of their ensemble averages, $\langle \Delta G_{ND}(\boldsymbol{\sigma})\rangle_{\boldsymbol{\sigma}}$, and the experimental values of $\Delta G_{ND}(\boldsymbol{\sigma}_N)$ listed in Table S4. The correlation in the case of $r_{\text{cutoff}} \sim 8$ Å is quite well, indicating that the constancy approximation (Eq. 11) for the variance of ΔG_N is appropriate.

The conformational entropy per residue in the compact denatured state, $\hat{\omega}$ in Eq. A18, estimated from the condition for the first order transition falls into the ranges of 0.6–1.1k_B for $r_{\text{cutoff}} \sim 8$Å and 0.8–1.4k_B for $r_{\text{cutoff}} \sim 15.5$Å . This range for $r_{\text{cutoff}} \sim 8$Å agrees well with the range estimated by Morcos et al. (11).

3 Discussion

We have analyzed the interaction changes ($\Delta\psi_N$) due to single nucleotide nonsynonymous substitutions. As studied in the succeeding manuscript (13), the regression coefficient of their mean ($\overline{\Delta\psi_N}$) on ψ_N must be more negative than that of their standard deviation (Sd($\Delta\psi_N$)), otherwise the folding free energy, $\Delta G_{ND} = k_B T_s \Delta\psi_{ND}$, of protein could not have a stable equilibrium value; actually Tables 2 and S5 show that their mean over all the substitutions at all sites is negatively proportional to ψ_N of a wildtype, but their standard deviation is nealy constant irrespective of ψ_N across homologous sequences.

On the basis of the random energy model(REM) (3), the effective temperatures (T_s) of natural selection, glass transition temperatures (T_g), and folding free energies (ΔG_{ND}) for 14 protein domains are estimated in the empirical approximation that the variance of $\Delta\psi_N$ is constant across homologous sequences with different ψ_N, so that their estimates may be coarse-grained, however, this method is easier and faster than the method (11) using the AWSEM (12). Experimental data for ΔG_{ND} are very limited, and also experimental conditions such as temperature and pH tend to be different among them. A prediction method for folding free energy would be useful in such a situation, although the present method requires the knowledge of melting temperature (T_m) besides sequence data, however, experimental data of T_m are more available than for ΔG_{ND}.

We have employed the cutoff distances for pairwise interactions, $r_{\text{cutoff}} \sim 8$ and 15.5Å , which correspond to the first and second interaction shells between residues, respectively. Also the ratio of pseudocount p_c was chosen to yield the sample and ensemble averages are equal, i.e., $\overline{\psi_N} = \langle \psi_N\rangle_{\boldsymbol{\sigma}}$. Morcos et al. (11) employed probably $p_c = 0.5$, which was successfully employed in contact prediction, and chose $r_{\text{cutoff}} = 16$Å on the basis of the correlation between $\Delta\Delta G_{ND}$ and $\Delta\Delta\psi_{ND} \simeq \Delta\psi_N$ due to single amino acid substitutions for the PDZ protein family. In the present method, $p_c = 0.5$ cannot be used, because

Fig. S1 shows that for $p_c = 0.5$, $\overline{\psi_N}$ coincides with $\langle\psi_N\rangle_{\boldsymbol{\sigma}}$ at $r_{\text{cutoff}} \simeq 8$Å in the Ising gauge but is more negative than $\langle\psi_N\rangle_{\boldsymbol{\sigma}}$ at any cutoff distance in the simple gauge. The condition of $\overline{\psi_N} = \langle\psi_N\rangle_{\boldsymbol{\sigma}}$ is required to estimate folding free energies ΔG_{ND} with Eq. A27 on the basis of the REM.

As shown in Fig. 3, the estimates of T_s depend on the cutoff distance. The estimates of T_s are determined in relative to T_s of the PDZ, which has been estimated to be equal to the reflective regression coefficient of experimental $\Delta\Delta G_{ND}$ on $\Delta\psi_N (\simeq \Delta\Delta\psi_{ND})$. Larger the variance of $\Delta\psi_N$ is, the smaller the estimate of T_s is. Including the longer range of pairwise interactions increases the variance of $\Delta\psi_N$. Correlation between $\Delta\psi_N$ and $\Delta\Delta G_{ND}$ is not a good measure to judge which cutoff distance is better. T_s is not directly observable. Comparison of the estimates of folding free energies with their experimental values may be appropriate to judge which value is more appropriate for the cutoff distance. It is not certain at this time which value better suits the present analysis, but consistencies between various quantities, particularly between $\langle\Delta G_{ND}\rangle_{\boldsymbol{\sigma}}$ and experimental ΔG_{ND}, may indicate that $r_{\text{cutoff}} \sim 8$Å slightly better suits the present method than $r_{\text{cutoff}} \sim 15.5$Å ; see Figs. 5 and 7.

4 Appendix

4.1 Knowledge of protein folding

A protein folding theory (3), which is based on a random energy model (REM), indicates that the equilibrium ensemble of amino acid sequences, $\boldsymbol{\sigma} = (\sigma_1, \cdots, \sigma_L)$ where σ_i is the type of amino acid at site i and L is sequence length, should be a canonical ensemble with a Boltzmann factor consisting of the folding free energy, $\Delta G_{ND}(\boldsymbol{\sigma}, T)$ and an effective temperature T_s of natural selection.

$$P(\boldsymbol{\sigma}) \propto P^{\text{mut}}(\boldsymbol{\sigma}) \exp(\frac{-\Delta G_{ND}(\boldsymbol{\sigma}, T)}{k_B T_s}) \tag{A1}$$

$$\propto \exp(\frac{-G_N(\boldsymbol{\sigma})}{k_B T_s}) \qquad \text{if } \boldsymbol{f}(\boldsymbol{\sigma}) = \text{constant} \tag{A2}$$

$$\Delta G_{ND}(\boldsymbol{\sigma}, T) \equiv G_N(\boldsymbol{\sigma}) - G_D(\boldsymbol{f}(\boldsymbol{\sigma}), T) \tag{A3}$$

where $p^{\text{mut}}(\boldsymbol{f}(\boldsymbol{\sigma}))$ is the probability of a sequence $(\boldsymbol{\sigma})$ randomly occurring in a mutational process and depends only on the amino acid frequencies $\boldsymbol{f}(\boldsymbol{\sigma})$, k_B is the Boltzmann constant, T is a growth temperature, and G_N and G_D are the free energies of the native conformation and denatured state, respectively. Selection temperature T_s quantifies how strong the folding constraints have been during evolution (11), and is specific to the protein structure and function. The free energy G_D of the denatured state does not depend on the amino acid order but the amino acid composition, $\boldsymbol{f}(\boldsymbol{\sigma})$, in a sequence. It is reasonable to assume that mutations independently occur between sites, and therefore the equilibrium frequency of a sequence in the mutational process is equal to the product of the equilibrium frequencies over sites; $P^{\text{mut}}(\boldsymbol{\sigma}) = \prod_i p^{\text{mut}}(\sigma_i)$, where $p^{\text{mut}}(\sigma_i)$ is the equilibrium frequency of σ_i at site i in the mutational process.

The distribution of conformational energies in the denatured state (molten globule state), which consists of conformations as compact as the native conformation. is approximated in the random energy model (REM), particularly the independent interaction model (IIM) (3), to be equal to the energy distribution of randomized sequences, which is then approximated by a Gaussian distribution, in the native conformation. That is, a partition function Z for the denatured state is written as follows with the energy density $n(E)$ of conformations that is approximated by a product of a Gaussian probability density and the total number of conformations whose logarithm is proportional to the chain length.

$$Z = \int \exp(\frac{-E}{k_B T})\, n(E) dE \tag{A4}$$

$$n(E) \approx \exp(\omega L) \mathcal{N}(\bar{E}(\boldsymbol{f}(\boldsymbol{\sigma})), \delta E^2(\boldsymbol{f}(\boldsymbol{\sigma}))) \tag{A5}$$

where ω is the conformational entropy per residue in the compact denatured state, and $\mathcal{N}(\bar{E}(\boldsymbol{f}(\boldsymbol{\sigma})), \delta E^2(\boldsymbol{f}(\boldsymbol{\sigma})))$ is the Gaussian probability density with mean $\bar{E}$ and variance δE^2, which depend only on the amino acid composition of the protein sequence. The free energy of the denatured state is approximated as follows.

$$G_D(\boldsymbol{f}(\boldsymbol{\sigma}), T) \approx \bar{E}(\boldsymbol{f}(\boldsymbol{\sigma})) - \frac{\delta E^2(\boldsymbol{f}(\boldsymbol{\sigma}))}{2 k_B T} - k_B T \omega L \tag{A6}$$

$$= \bar{E}(\boldsymbol{f}(\boldsymbol{\sigma})) - \delta E^2(\boldsymbol{f}(\boldsymbol{\sigma})) \frac{\vartheta(T/T_g)}{k_B T} \tag{A7}$$

$$\vartheta(T/T_g) \equiv \begin{cases} \frac{1}{2}(1 + \frac{T^2}{T_g^2}) & \text{for } T > T_g \\ \frac{T}{T_g} & \text{for } T \le T_g \end{cases} \tag{A8}$$

where $\bar{E}$ and δE^2 are estimated as the mean and variance of interaction energies of randomized sequences in the native conformation. T_g is the glass transition temperature of the protein at which entropy becomes zero (3); $-\partial G_D/\partial T|_{T=T_g} = 0$. The conformational entropy per residue ω in the compact denatured state can be represented with T_g; $\omega L = \delta E^2/(2(k_B T_g)^2)$. Thus, unless $T_g < T_m$, a protein will be trapped at local minima on a rugged free energy landscape before it can fold into a unique native structure.

4.2 Probability distribution of homologous sequences in sequence space

The probability distribution $P(\boldsymbol{\sigma})$ of sequences, $\boldsymbol{\sigma} \equiv (\sigma_1, \cdots, \sigma_L)$ where $\sigma_i \in$ {amino acids, deletion}, with maximum entropy in sequence space that satisfies a given amino acid frequency at each site and a given pairwise amino acid frequency at each site pair is a Boltzmann distribution (4, 5).

$$P(\boldsymbol{\sigma}) \propto \exp(-\psi_N(\boldsymbol{\sigma})) \tag{A9}$$

$$\psi_N(\boldsymbol{\sigma}) \equiv -(\sum_{i}^{L}(h_i(\sigma_i) + \sum_{j>i} J_{ij}(\sigma_i, \sigma_j))) \tag{A10}$$

where h_i and J_{ij} are one-body and two-body interactions and must satisfy the following constraints.

$$\sum_{\boldsymbol{\sigma},\sigma_i=a_k} P(\boldsymbol{\sigma}) = P_i(a_k) \tag{A11}$$

$$\sum_{\boldsymbol{\sigma},\sigma_i=a_k,\sigma_j=a_l} P(\boldsymbol{\sigma}) = P_{ij}(a_k, a_l) \tag{A12}$$

where $P_i(a_k)$ is the frequency of amino acid a_k at site i and $P_{ij}(a_k, a_l)$ is the frequency of amino acid pair, a_k at i and a_l at j; $a_k \in$ {amino acids, deletion}. The pairwise interaction matrix J satisfies $J_{ij}(a_k, a_l) = J_{ji}(a_l, a_k)$ and $J_{ii}(a_k, a_l) = 0$. Interactions h_i and J_{ij} can be well estimated from a multiple sequence alignment (MSA) in the mean field approximation (4, 5), or by maximizing a pseudo-likelihood (6, 7). Here we must notice that $\psi_N(\boldsymbol{\sigma})$ has been estimated under the constraints on amino acid compositions at all sites, and therefore the amino acid composition of a whole sequence must be constant across sequences.

From Eqs. A2 and A9,

$$G_N(\boldsymbol{\sigma}) = k_B T_s[\,\psi_N(\boldsymbol{\sigma}) + \text{function of}\boldsymbol{f}(\boldsymbol{\sigma})\,] \tag{A13}$$

$$G_D(\boldsymbol{f}(\boldsymbol{\sigma}), T) = k_B T_s[\,\psi_D(\boldsymbol{\sigma}) + \text{function of}\boldsymbol{f}(\boldsymbol{\sigma})\,] \tag{A14}$$

$$\Delta G_{ND}(\boldsymbol{\sigma}, T) = k_B T_s\, \Delta\psi_{ND}(\boldsymbol{\sigma}) \tag{A15}$$

$$\Delta\psi_{ND}(\boldsymbol{\sigma}) \equiv \psi_N(\boldsymbol{\sigma}) - \psi_D(\boldsymbol{\sigma}) \tag{A16}$$

$$\psi_D(\boldsymbol{\sigma}) \approx \bar{\psi}(\boldsymbol{f}(\boldsymbol{\sigma})) - \delta\psi^2(\boldsymbol{f}(\boldsymbol{\sigma}))\vartheta(T/T_g)T_s/T \tag{A17}$$

$$\omega = (T_s/T_g)^2\delta\psi^2/(2L) \tag{A18}$$

where $\bar{E} = k_B T_s\bar{\psi}$ and $\delta E^2 = (k_B T_s)^2\delta\psi^2$. The mean $\bar{\psi}$ and variance $\Delta\psi^2$ are estimated as the mean and variance of ψ_N over randomized sequences in the native structure (3).

4.3 The ensemble average of folding free energy, $\Delta G_{ND}(\boldsymbol{\sigma}, T)$, over sequences

The ensemble average of $\Delta G_{ND}(\boldsymbol{\sigma}, T)$ over sequences with Eq. A1 is

$$\langle \Delta G_{ND}(\boldsymbol{\sigma}, T)\rangle_{\boldsymbol{\sigma}} \tag{A19}$$

$$\equiv [\sum_{\boldsymbol{\sigma}} \Delta G_{ND}(\boldsymbol{\sigma}, T)P^{\text{mut}}(\boldsymbol{\sigma})\exp(-\frac{\Delta G_{ND}(\boldsymbol{\sigma}, T)}{k_B T_s})\,] / [\sum_{\boldsymbol{\sigma}} P^{\text{mut}}(\boldsymbol{\sigma})\exp(-\frac{\Delta G_{ND}(\boldsymbol{\sigma}, T)}{k_B T_s})\,] \tag{A20}$$

$$\approx [\sum_{\boldsymbol{\sigma}\,|\,\boldsymbol{f}(\boldsymbol{\sigma})=\overline{\boldsymbol{f}(\boldsymbol{\sigma}_N)}} G_N(\boldsymbol{\sigma})\exp(-\frac{G_N(\boldsymbol{\sigma})}{k_B T_s})\,] / [\sum_{\boldsymbol{\sigma}\,|\,\boldsymbol{f}(\boldsymbol{\sigma})=\overline{\boldsymbol{f}(\boldsymbol{\sigma}_N)}} \exp(-\frac{G_N(\boldsymbol{\sigma})}{k_B T_s})\,] - G_D(\overline{\boldsymbol{f}(\boldsymbol{\sigma}_N)}, T) \tag{A21}$$

$$= \langle G_N(\boldsymbol{\sigma})\rangle_{\boldsymbol{\sigma}} - G_D(\overline{\boldsymbol{f}(\boldsymbol{\sigma}_N)}, T) \tag{A22}$$

where $\boldsymbol{\sigma}_N$ denotes a native sequence, and $\overline{\boldsymbol{f}(\boldsymbol{\sigma}_N)}$ denotes the average of $\boldsymbol{f}(\boldsymbol{\sigma}_N)$ over homologous sequences. In Eq. A21, the sum over all sequences is approximated by the sum over sequences the amino acid composition of which is the same as that of the native sequences. The ensemble average of G_N is also estimated in the Gaussian approximation (3).

$$\langle G_N(\boldsymbol{\sigma})\rangle_{\boldsymbol{\sigma}} \approx \frac{\int E \exp(-E/(k_B T_s))\, n(E)\, dE}{\int \exp(-E/(k_B T_s))\, n(E)\, dE} \tag{A23}$$

$$= \bar{E}(\overline{\boldsymbol{f}(\boldsymbol{\sigma}_N)}) - \delta E^2(\overline{\boldsymbol{f}(\boldsymbol{\sigma}_N)})/(k_B T_s) \tag{A24}$$

$$\langle \psi_N(\boldsymbol{\sigma})\rangle_{\boldsymbol{\sigma}} \approx \bar{\psi}(\overline{\boldsymbol{f}(\boldsymbol{\sigma}_N)}) - \delta\psi^2(\overline{\boldsymbol{f}(\boldsymbol{\sigma}_N)}) \tag{A25}$$

The ensemble averages of $\Delta G_{ND}(\boldsymbol{\sigma}, T)$ and $\psi_N(\boldsymbol{\sigma})$ over sequences are observable as the sample averages of $\Delta G_{ND}(\boldsymbol{\sigma}_N, T_s)$ and $\psi_N(\boldsymbol{\sigma}_N)$ over homologous sequences fixed in protein evolution, respectively.

$$\overline{\Delta G_{ND}(\boldsymbol{\sigma}_N, T)} = \langle \Delta G_{ND}(\boldsymbol{\sigma}, T)\rangle_{\boldsymbol{\sigma}} \tag{A26}$$

$$\approx k_B T_s \delta\psi^2(\overline{\boldsymbol{f}(\boldsymbol{\sigma}_N)})\, [\, \vartheta(T/T_g) T_s/T - 1\,] \tag{A27}$$

$$\overline{\psi_N(\boldsymbol{\sigma}_N)} \equiv \frac{\sum_{\boldsymbol{\sigma}_N} w_{\boldsymbol{\sigma}_N} \psi_N(\boldsymbol{\sigma}_N)}{\sum_{\boldsymbol{\sigma}_N} w_{\boldsymbol{\sigma}_N}} \tag{A28}$$

$$= \langle \psi_N(\boldsymbol{\sigma})\rangle_{\boldsymbol{\sigma}} \tag{A29}$$

where the overline denotes sample average with a sample weight $w_{\boldsymbol{\sigma}_N}$ for each homologous sequence, which is used to reduce phylogenetic biases in the set of homologous sequences.

The folding free energy becomes equal to zero at the melting temperature T_m; $\langle \Delta G_{ND}(\boldsymbol{\sigma}_N, T_m)\rangle_{\boldsymbol{\sigma}} = 0$. Thus, the following relationship must be satisfied (3).

$$\vartheta(T_m/T_g)\frac{T_s}{T_m} = \frac{T_s}{2T_m}\left(1 + \frac{T_m^2}{T_g^2}\right) = 1 \quad \text{with } T_s \le T_g \le T_m \tag{A30}$$

5 Supporting Citation

References (20–36) appear in the Supporting Material.

SUPPLEMENTARY MATERIAL

An online supplement to this article can be found by visiting BJ Online at http://www.biophysj.org.

References

1. Bryngelson, J. D., and P. G. Wolynes, 1987. Spin glasses and the statistical mechanics of protein folding. Proc. Natl. Acad. Sci. USA 84:7524–7528.
2. Ramanathan, S., and E. Shakhnovich, 1994. Statistical mechanics of proteins with evolutionary selected sequences. Phys. Rev. E 50:1303–1312.
3. Pande, V. S., A. Y. Grosberg, and T. Tanaka, 1997. Statistical mechanics of simple models of protein folding and design. Biophys. J. 73:3192–3210.
4. Morcos, F., A. Pagnani, B. Lunt, A. Bertolino, D. S. Marks, C. Sander, R. Zecchina, J. N. Onuchic, T. Hwa, and M. Weigt, 2011. Direct-coupling analysis of residue coevolution captures native contacts across many protein families. Proc. Natl. Acad. Sci. USA 108:E1293–E1301.
5. Marks, D. S., L. J. Colwell, R. Sheridan, T. A. Hopf, A. Pagnani, R. Zecchina, and C. Sander, 2011. Protein 3D Structure Computed from Evolutionary Sequence Variation. PLoS ONE 6:e28766. http://dx.doi.org/10.1371/journal.pone.0028766.
6. Ekeberg, M., C. Lövkvist, Y. Lan, M. Weigt, and E. Aurell, 2013. Improved contact prediction in proteins: Using pseudolikelihoods to infer Potts models. Phys. Rev. E 87:012707–1–16. http://link.aps.org/doi/10.1103/PhysRevE.87.012707.
7. Ekeberg, M., T. Hartonen, and E. Aurell, 2014. Fast pseudolikelihood maximization for direct-coupling analysis of protein structure from many homologous amino-acid sequences. J. Comput. Phys. 276:341–356.
8. Miyazawa, S., 2013. Prediction of Contact Residue Pairs Based on Co-Substitution between Sites in Protein Structures. PLoS ONE 8:e54252. http://dx.doi.org/10.1371/journal.pone.0054252.
9. Sułkowska, J. I., F. Morcos, M. Weigt, T. Hwa, and J. N. Onuchic, 2012. Genomics-aided structure prediction. Proc. Natl. Acad. Sci. USA 109:10340–10345.

10. Hopf, T. A., L. J. Colwell, R. Sheridan, B. Rost, C. Sander, and D. S. Marks, 2012. Three-Dimensional Structures of Membrane Proteins from Genomic Sequencing. Cell 149:1607–1621.
11. Morcos, F., N. P. Schafer, R. R. Cheng, J. N. Onuchic, and P. G. Wolynes, 2014. Coevolutionary information, protein folding landscapes, and the thermodynamics of natural selection. Proc. Natl. Acad. Sci. USA 111:12408–12413.
12. Davtyan, A., N. P. Schafer, W. Zheng, C. Clementi, P. G. Wolynes, , and G. A. Papoian, 2012. AWSEM-MD: Protein Structure Prediction Using Coarse-Grained Physical Potentials and Bioinformatically Based Local Structure Biasing. J. Phys. Chem. B 116:8494–8503.
13. Miyazawa, S., 2016. Selection originating from protein foldability: Folding free energy, sequence ensemble, and fitness .
14. Finn, R., P. Coggill, R. Y. Eberhardt, S. R. Eddy, J. Mistry, A. L. Mitchell, S. C. Potter, M. Punta, M. Qureshi, A. Sangrador-Vegas, G. A. Salazar, and A. B. J. Tate, 2016. The Pfam protein families database; towards a more sustainable future. Nucl. Acid Res. 44:D279–D285.
15. Gianni, S., C. D. Geierhaas, N. Calosci, P. Jemth, G. W. Vuister, C. Travaglini-Allocatelli, M. Vendruscolo, and M. Brunori, 2007. A PDZ domain recapitulates a unifying mechanism for protein folding. Proc. Natl. Acad. Sci. USA 104:128–133.
16. Tokuriki, N., F. Stricher, J. Schymkowitz, L. Serrano, and D. S. Tawfik, 2007. The Stability Effects of Protein Mutations Appear to be Universally Distributed. J. Mol. Biol. 369:1318–1332.
17. Serohijos, A., Z. Rimas, and E. Shakhnovich, 2012. Protein Biophysics Explains Why Highly Abundant Proteins Evolve Slowly. Cell Reports 2:249 – 256. http://dx.doi.org/10.1016/j.celrep.2012.06.022.
18. Onuchic, J. N., P. G. Wolynes, Z. Lutheyschulten, and N. D. Socci, 1995. Toward an outline of the topography of a realistic protein-folding funnel. Proc. Natl. Acad. Sci. USA 92:3626–3630.
19. Pande, V. S., A. Y. Grosberg, and T. Tanaka, 2000. Heteropolymer freezing and design: Towards physical models of protein folding. Rev. Mod. Phys. 72:259–314.
20. Ganguly, T., M. Das, A. Bandhu, P. K. Chanda, B. Jana, R. Mondal, and S. Sau, 2009. Physicochemical properties and distinct DNA binding capacity of the repressor of temperate Staphylococcus aureus phage ϕ/11. FEBS J. 276:1975–1985.
21. Wilson, C. J., and P. Wittung-Stafshede, 2005. Snapshots of a Dynamic Folding Nucleus in Zinc-Substituted Pseudomonas aeruginosa Azurin. Biochemistry 44:10054–10062.
22. Ruiz-Sanz, J., A. Simoncsits, I. Tőrő, S. Pongor, P. L. Mateo, and V. V. Filimonov, 1999. A thermodynamic study of the 434-repressor N-terminal domain and of its covalently linked dimers. Eur. J. Biochem 263:246–253.
23. Stupák, M., G. Zŏldák, A. Musatov, M. Sprinzl, and E. Sedlák, 2006. Unusual effect of salts on the homodimeric structure of NADH oxidase from *Thermus thermophilus* in acidic pH. Biochim. Biophys. Acta 1764:129–137.
24. D'Auria, S., A. Scirè, A. Varriale, V. Scognamiglio, M. Staiano, A. Ausili, A. Marabotti, MosèRossi, and F. Tanfani, 2005. Binding of Glutamine to Glutamine-Binding Protein from *Escherichia coli* Induces Changes in Protein Structure and Increases Protein Stability. Proteins 58:80–87.
25. Parsons, L. M., F. Lin, and J. Orban, 2006. Peptidoglycan Recognition by Pal, an Outer Membrane Lipoprotein. Biochemistry 45:2122–2128.
26. Williams, N. K., P. Prosselkov, E. Liepinsh, I. Line, A. Sharipo, D. R. Littler, P. M. G. Curmi, G. Otting, and N. E. Dixon, 2002. *In Vivo* Protein Cyclization Promoted by a Circularly Permuted *Synechocystis* sp. PCC6803 DnaB Mini-intein. J. Biol. Chem. 277:7790–7798.
27. Sainsbury, S., J. Ren, N. J. Saunders, D. I. Stuarta, and R. J. Owens, 2008. Crystallization and preliminary X-ray analysis of CrgA, a LysR-type transcriptional regulator from pathogenic *Neisseria meningitidis* MC58. Acta Cryst. F64:797–801.
28. Armengaud, J., J. Urbonavicius, B. Fernandez, G. Chaussinand, J. M. Bujnicki, and H. Grosjean, 2004. N^2-Methylation of Guanosine at Position 10 in tRNA Is Catalyzed by a THUMP Domain-containing, S-Adenosylmethionine-dependent Methyltransferase, Conserved in Archaea and Eukaryota. JBiolChem 279:37142–37152.
29. Guelorget, A., M. Roovers, V. Guérineau, C. Barbey, X. Li, , and B. Golinelli-Pimpaneau, 2010. Insights into the hyperthermostability and unusual region-specificity of archaeal *Pyrococcus abyssi* tRNA m^1A57/58 methyltransferase. Nucl. Acid Res. 38:6206–6218.
30. Knapp, S., P. T. Mattson, P. Christova, K. D. Berndt, A. Karshikoff, M. Vihinen, C. E. Smith, and R. Ladenstein, 1998. Thermal Unfolding of Small Proteins With SH3 Domain Folding Pattern. Proteins 31:309–319.
31. Grantcharova, V. P., D. S. Riddle, J. V. Santiago, and D. Baker, 1998. Important role of hydrogen bonds in the structurally polarized transition state for folding of the src SH3 domain. Nature Struct. Biol 714–720.
32. Onwukwe, G. U., P. Kursula1, M. K. Koski, W. Schmitz, and R. K. Wierenga, 2014. Human Δ^3,Δ^2-enoyl-CoA isomerase, type 2: a structural enzymology study on the catalytic role of its ACBP domain and helix-10. FEBS J. 282:746–768.
33. Kragelund, B. B., P. Osmark, T. B. Neergaard, J. Schiødt, K. Kristiansen, J. Knudsen, and F. M. Poulsen, 1999. The formation of a native-like structure containing eight conserved hydrophobic residues is rate limiting in two-state protein folding of ACBP. Nature Struct. Biol 6:594–601.
34. Torchio, G. M., M. R. Ermácora, and M. P. Sica, 2012. Equilibrium Unfolding of the PDZ Domain of β2-Syntrophin. Biophys. J. 102:2835–2844.
35. Gianni, S., N. Calosci1, J. M. A. Aelen, G. W. Vuister, M. Brunori, and C. Travaglini-Allocatelli, 2005. Kinetic folding mechanism of PDZ2 from PTP-BL. Protein Eng. Design Selection 18:389–395.
36. Rosa, C. L., D. Milardi, D. Grasso, R. Guzzi, and L. Sportelli, 1995. Thermodynamics of the Thermal Unfolding of Azurin. J. Phys. Chem. 99:14864–14870.

Table 1: **Protein families, and structures studied.**

Pfam family	UniProt ID	N [a]	N_{eff} [bc]	M [d]	M_{eff} [ce]	L [f]	PDB ID
HTH_3	RPC1_BP434/7-59	15315(15917)	11691.21	6286	4893.73	53	1R69-A:6-58
Nitroreductase	Q97IT9_CLOAB/4-76	6008(6084)	4912.96	1057	854.71	73	3E10-A/B:4-76
SBP_bac_3 [g]	GLNH_ECOLI/27-244	9874(9972)	7374.96	140	99.70	218	1WDN-A:5-222
SBP_bac_3	GLNH_ECOLI/111-204	9712(9898)	7442.85	829	689.64	94	1WDN-A:89-182
OmpA	PAL_ECOLI/73-167	6035(6070)	4920.44	2207	1761.24	95	1OAP-A:52-146
DnaB	DNAB_ECOLI/31-128	1929(1957)	1284.94	1187	697.30	98	1JWE-A:30-127
LysR_substrate [g]	BENM_ACIAD/90-280	25138(25226)	20707.06	85(1)	67.00	191	2F6G-A/B:90-280
LysR_substrate	BENM_ACIAD/163-265	25032(25164)	21144.74	121(1)	99.27	103	2F6G-A/B:163-265
Methyltransf_5 [g]	RSMH_THEMA/8-292	1942(1953)	1286.67	578(2)	357.97	285	1N2X-A:8-292
Methyltransf_5	RSMH_THEMA/137-216	1877(1911)	1033.35	975(2)	465.53	80	1N2X-A:137-216
SH3_1	SRC_HUMAN:90-137	9716(16621)	3842.47	1191	458.31	48	1FMK-A:87-134
ACBP	ACBP_BOVIN/3-82	2130(2526)	1039.06	161	70.72	80	2ABD-A:2-81
PDZ	PTN13_MOUSE/1358-1438	13814(23726)	4748.76	1255	339.99	81	1GM1-A:16-96
Copper-bind	AZUR_PSEAE:24-148	1136(1169)	841.56	67(1)	45.23	125	5AZU-A/B/C/D:4-128

[a] The number of unique sequences and the total number of sequences in parentheses; the full alignments in the Pfam (14) are used.
[b] The effective number of sequences.
[c] A sample weight (w_{σ_N}) for a given sequence is equal to the inverse of the number of sequences that are less than 20% different from the given sequence.
[d] The number of unique sequences that include no deletion unless specified. The number in parentheses indicates the maximum number of deletions allowed.
[e] The effective number of unique sequences that include no deletion or at most the specified number of deletions.
[f] The number of residues.
[g] These proteins consist of two domains, and other ones are single domains.

Table 2: **Parameter values for $r_{\mathbf{cutoff}} \sim 8$ Å** employed for each protein family, and the averages of the total interactions ($\overline{\overline{\psi_N}}$) over all homologous sequences and of the means and the variances of interaction changes ($\overline{\overline{\Delta\psi_N}}$ and $\overline{\mathrm{Var}(\Delta\psi_N)}$) due to single nucleotide nonsynonymous mutations at all sites over all homologous sequences in each protein family.

Pfam family	L	p_c	n_c [a]	r_{cutoff} (Å)	$\bar{\psi}/L$ [b]	$\delta\psi^2/L$ [b]	$\overline{\psi_N}/L$ [b]	$\overline{\overline{\Delta\psi_N}}$ [c]	$\overline{\mathrm{Var}(\Delta\psi_N)}$ [c]	r_{ψ_N} for $\overline{\overline{\Delta\psi_N}}$ [d]	α_{ψ_N}	r_{ψ_N} for $(\mathrm{Var}(\Delta\psi_N))^{1/2}$ [e]	α_{ψ_N}
HTH_3	53	0.175	7.434	8.22	−0.2039	2.8837	−3.0712	4.0412	30.8500	−0.94	−1.3671	−0.23	−0.1741
Nitroreductase	73	0.24	6.411	8.39	−0.1153	2.0825	−2.1975	2.9168	11.0879	−0.94	−1.3915	−0.59	−0.5270
SBP_bac_3	218	0.25	9.230	8.10	−0.1000	2.1624	−2.2618	3.1534	12.2140	−0.98	−1.5267	−0.84	−0.8111
SBP_bac_3	94	0.37	8.000	7.90	−0.1634	1.2495	−1.4054	1.8075	5.6101	−0.96	−1.4191	−0.65	−0.5171
OmpA	95	0.169	8.000	8.20	−0.2457	3.9093	−4.1542	6.0657	55.3105	−0.96	−1.5882	−0.47	−0.4471
DnaB	98	0.235	9.653	8.17	−0.2284	3.9976	−4.2291	6.1006	38.5736	−0.96	−1.4654	−0.52	−0.4385
LysR_substrate	191	0.23	7.843	7.87	−0.2248	1.4450	−1.6712	1.9999	6.7385	−0.97	−1.3646	−0.52	−0.5814
LysR_substrate	103	0.265	8.835	8.25	−0.2240	1.4132	−1.6372	2.0309	7.4763	−0.99	−1.4629	−0.78	−0.6311
Methyltransf_5	285	0.13	7.993	7.78	−0.1462	7.2435	−7.3887	12.2738	127.1400	−0.99	−1.7945	−0.08	−0.0461
Methyltransf_5	80	0.18	6.775	7.85	−0.1763	5.5162	−5.6896	8.7386	61.5293	−0.96	−1.5601	0.06	0.0612
SH3_1	48	0.14	6.417	8.01	−0.1348	3.9109	−4.0434	5.4273	39.8445	−0.94	−1.4457	−0.22	−0.1995
ACBP	80	0.22	9.175	8.24	−0.0525	4.6411	−4.7084	7.8272	55.1762	−0.97	−1.6189	−0.30	−0.1986
PDZ	81	0.205	9.061	8.16	−0.2398	3.1140	−3.3572	4.3897	21.0789	−0.96	−1.5014	−0.43	−0.3293
Copper-bind	125	0.23	9.232	8.26	−0.0838	4.1946	−4.2657	7.2514	51.7793	−0.98	−1.9254	−0.20	−0.1475

[a] The average number of contact residues per site within the cutoff distance; the center of side chain is used to represent a residue.
[b] M unique sequences without deletions are used with a sample weight (w_{σ_N}) for each sequence; w_{σ_N} is equal to the inverse of the number of sequences that are less than 20% different from a given sequence. The M and the effective number M_{eff} of the sequences are listed for each protein family in Table 1.
[c] Representatives of unique sequences without deletions, which are at least 20% different from each other, are used; the number of the representatives used is almost equal to M_{eff}. For HTH_3, 4431 sequences are used; abnormal sequences are removed.
[d] The correlation and regression coefficients of $\overline{\Delta\psi_N}$ on ψ_N/L;see Eq. 6.
[e] The correlation and regression coefficients of $(\mathrm{Var}(\Delta\psi_N))^{1/2}$ on ψ_N/L.

Table 3: **Thermodynamic quantities estimated with $r_{\mathbf{cutoff}} \sim 8$ Å .**

Pfam family	r [a]	$k_B\hat{T}_s$ [a] (kcal/mol)	$\hat{T}_s$ (°K)	experimental T_m (°K)	$\hat{T}_g$ (°K)	T [b] (°K)	$\hat{\omega}$ [c] (k_B)	$\langle\Delta G_{ND}\rangle$ [d] (kcal/mol)
HTH_3	-	-	116.3	343.7	155.1	298	0.8107	−2.98
Nitroreductase	-	-	194.0	337.0	214.2	298	0.8537	−2.62
SBP_bac_3	-	-	184.8	336.1	207.0	298	0.8622	−8.14
SBP_bac_3	-	-	272.7	336.1	277.7	298	0.6025	−0.99
OmpA	-	-	86.9	320.0	126.8	298	0.9171	−3.16
DnaB	-	-	104.0	312.8	139.7	298	1.1082	−2.52
LysR_substrate	-	-	248.8	338.0	258.0	298	0.6722	−3.46
LysR_substrate	-	-	236.2	338.0	247.7	298	0.6425	−2.05
Methyltransf_5	-	-	57.3	375.0	107.8	298	1.0220	−39.91
Methyltransf_5	-	-	82.3	375.0	131.7	298	1.0783	−11.14
SH3_1	0.86	0.1583	102.3	344.0	143.8	295	0.9904	−3.68
ACBP	0.82	0.1169	87.0	324.4	127.6	278	1.0774	−6.51
PDZ	0.93	0.2794	140.7	312.9	168.5	298	1.0854	−1.81
Copper-bind	0.83	0.1781	89.8	359.3	135.8	298	0.9171	−11.55

[a] Reflective correlation (r) and regression ($k_B\hat{T}_s$) coefficients for least-squares regression lines of experimental $\Delta\Delta G_{ND}$ on $\Delta\psi_N$ through the origin.
[b] Temperatures are set up for comparison to be equal to the experimental temperatures for ΔG_{ND} or to 298°K if unavailable; see Table S4 for the experimental data.
[c] Conformational entropy per residue, in k_B units, in the denatured molten-globule state; see Eq. A18.
[d] Folding free energy in kcal/mol units; see Eq. A27.

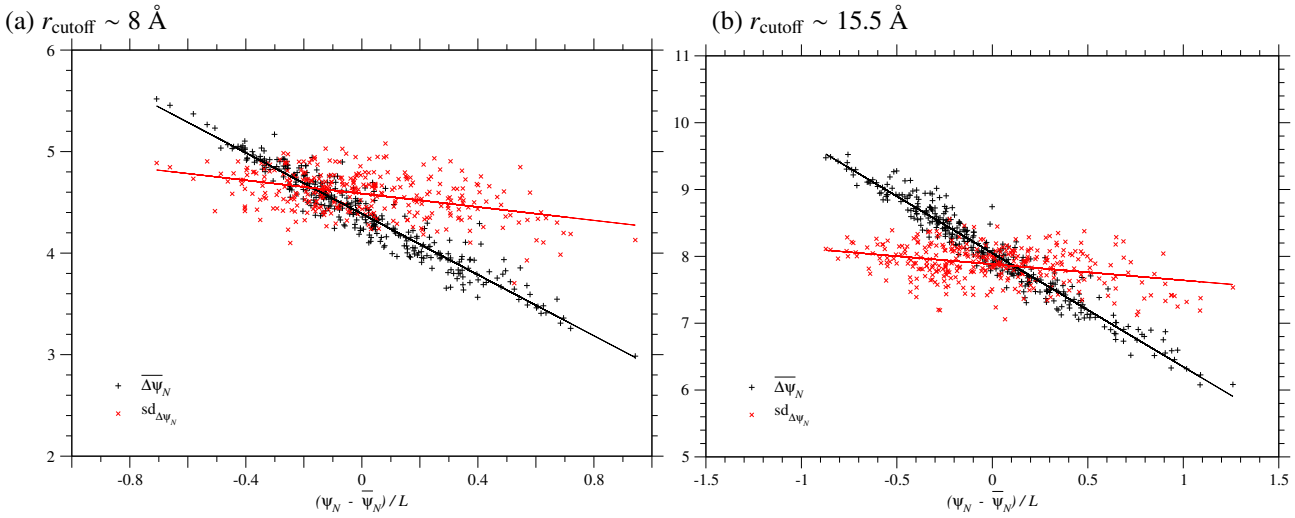


Figure 1: **Correlation between $\Delta\psi_N$ due to single nucleotide nonsynonymous substitutions and ψ_N of homologous sequences in the PDZ domain family.** The left and right figures correspond to the cutoff distance r_{cutoff} ~ 8 and 15.5Å respectively. Each of the black plus or red cross marks corresponds to the mean or the standard deviation of $\Delta\psi_N$ due to all types of single nucleotide nonsynonymous substitutions over all sites in each of the homologous sequences of the PDZ domain family. Only 335 representatives of unique sequences with no deletion, which are at least 20% different from each other, are employed; the number of the representatives is almost equal to M_{eff} in Table 1. The solid lines show the regression lines for the mean and the standard deviation of $\Delta\psi_N$.

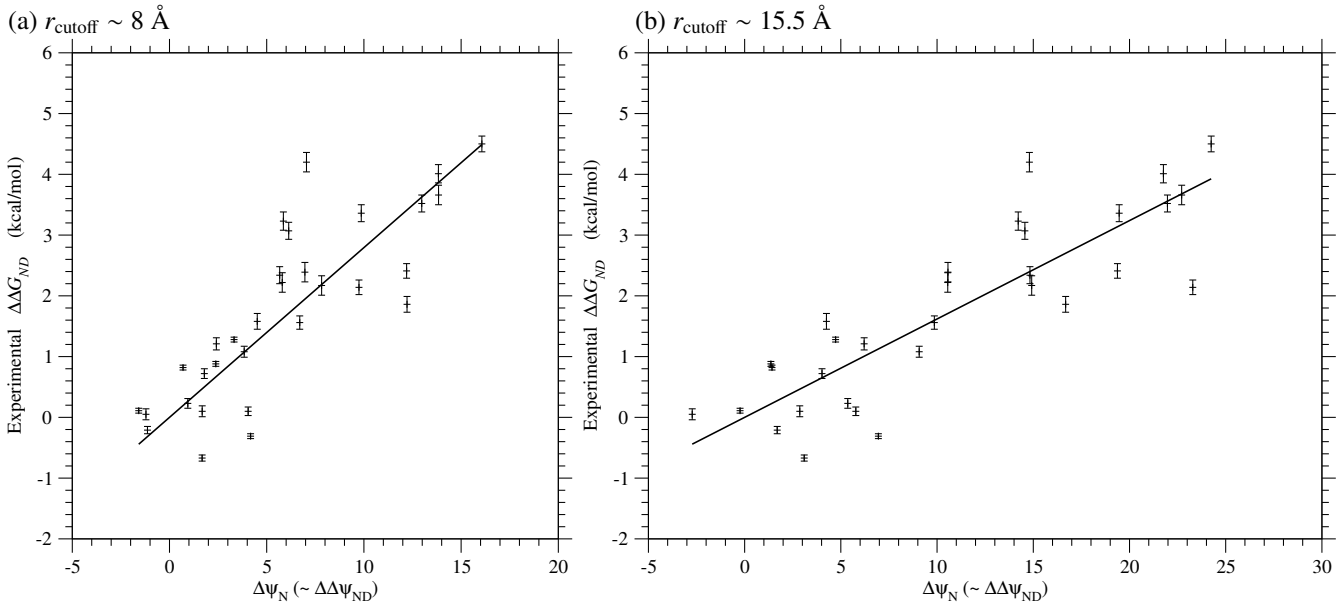


Figure 2: **Regression of the experimental values (15) of folding free energy changes ($\Delta\Delta G_{ND}$) due to single amino acid substitutions on $\Delta\psi_N(\simeq \Delta\Delta\psi_{ND})$ for the same types of substitutions in the PDZ domain.** The left and right figures correspond to the cutoff distance r_{cutoff} ~ 8 and 15.5Å respectively. The solid lines show the least-squares regression lines through the origin with the slopes, 0.279 kcal/mol for r_{cutoff} ~ 8Å and 0.162 kcal/mol for r_{cutoff} ~ 15.5 Å , which are the estimates of k_BT_s. The reflective correlation coefficients for them are equal to 0.93 and 0.94, respectively. The free energies are in kcal/mol units.

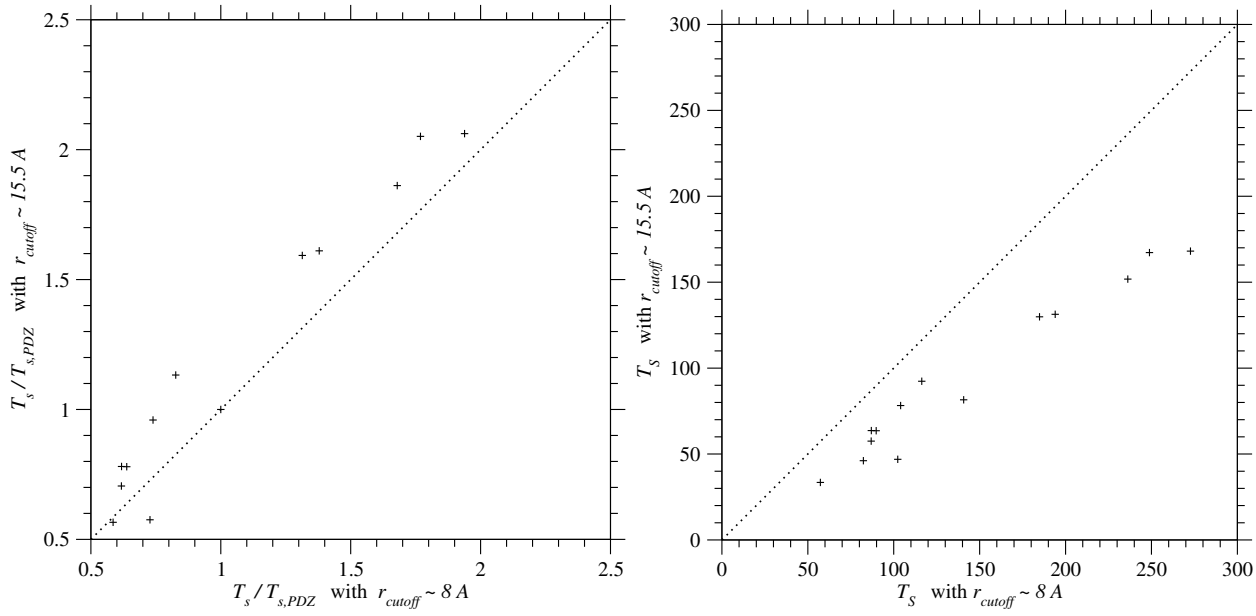


Figure 3: **Comparison of selection temperatures (T_s) estimated with different cutoff distances by the present method.** The abscissa and ordinate correspond to the cases of $r_{\text{cutoff}} \sim 8$ and 15.5Å respectively. The T_s is in °K units.

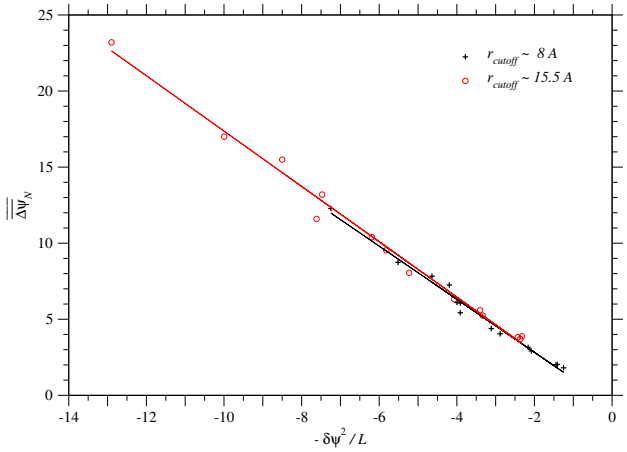


Figure 4: **Dependence of the average of $\overline{\Delta\psi_N}$ due to single nucleotide nonsynonymous substitutions over homologous sequences on $-\delta\psi^2/L$ across protein families.** Plus and open circle marks indicate the values for each protein family in the cases of $r_{\rm cutoff} \sim 8$ and 15.5Å, respectively. In the case of the cutoff distance 8 Å, the correlation coefficient is equal to 0.99, and the regression line is $\overline{\overline{\Delta\psi_N(\sigma^N_{j\neq i}, \sigma^N_i \to \sigma_i)}} = -1.75(-\delta\psi^2/L) - 0.67$. In the case of $r_{\rm cutoff} \sim 16$Å, the correlation coefficient is equal to 0.995, and the regression line is $\overline{\overline{\Delta\psi_N(\sigma^N_{j\neq i}, \sigma^N_i \to \sigma_i)}} = -1.82(-\delta\psi^2/L) - 0.81$.

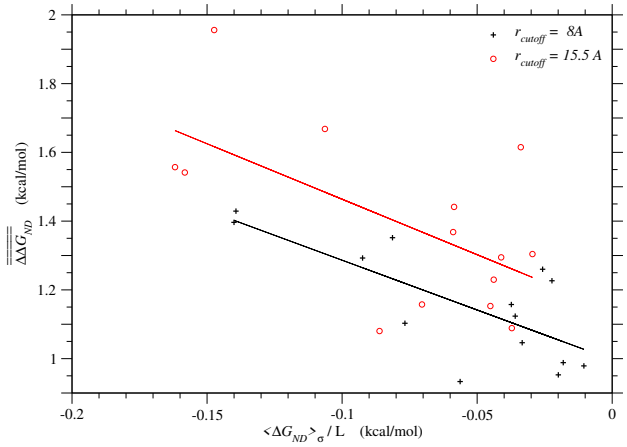


Figure 5: **The sample average of folding free energy change, $\overline{\overline{\Delta\Delta G_{ND}}} = k_B T_s \overline{\overline{\Delta\Delta\psi_{ND}}}$, is plotted against the ensemble average of folding free energy per residue, $\langle\Delta G_{ND}\rangle_{\boldsymbol{\sigma}}/L = k_B T_s \langle\Delta\psi_{ND}\rangle_{\boldsymbol{\sigma}}/L$, for each protein family.** In the case of the cutoff distance 8 Å, the correlation coefficient is $r = -0.74$, and the regression line is $\overline{\Delta\Delta G_{ND}(\sigma^N_{j\neq i}, \sigma^N_i \to \sigma_i)} = -2.90\langle\Delta G_{ND}\rangle_{\boldsymbol{\sigma}}/L + 1.00$. In the case of $r_{\text{cutoff}} \sim 16$ Å, the correlation coefficient is $r = -0.60$, and the regression line is $\overline{\Delta\Delta G_{ND}(\sigma^N_{j\neq i}, \sigma^N_i \to \sigma_i)} = -3.23\langle\Delta G_{ND}\rangle_{\boldsymbol{\sigma}}/L + 1.14$. The free energies are in kcal/mol units.

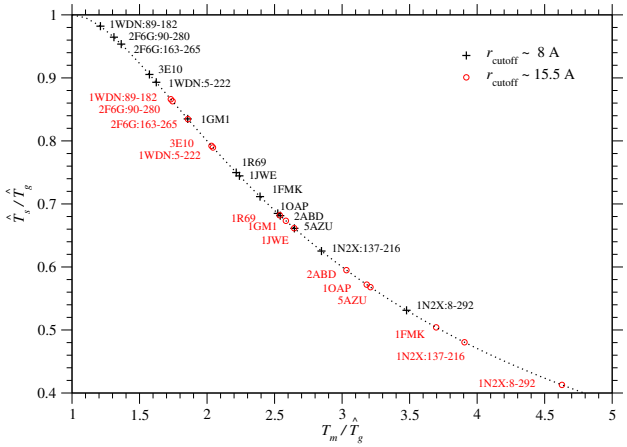


Figure 6: $\hat{T}_s/\hat{T}_g$ **is plotted against** $T_m/\hat{T}_g$ **for each protein domain.** A dotted curve corresponds to Eq. A30, $\hat{T}_s/\hat{T}_g = 2(T_m/\hat{T}_g)/((T_m/\hat{T}_g)^2 + 1)$. Plus and open circle marks indicate the values estimated with $r_{\text{cutoff}} \sim 8$ and 15.5Å , respectively. The T_s and T_g must satisfy $T_s < T_g < T_m$ for proteins to be able to fold into unique native structures.

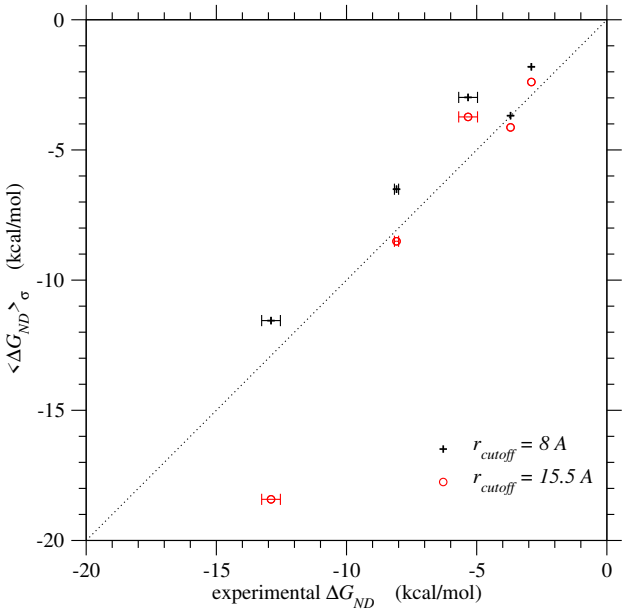


Figure 7: **Folding free energies, $\langle \Delta G_{ND} \rangle_\sigma$, predicted by the present method are plotted against their experimental values, $\Delta G_{ND}(\sigma_N)$.** The free energies are in kcal/mol units.

Supplementary material
for
"Selection originating from protein foldability:
I. A new method to estimate selection temperature"

Sanzo Miyazawa
sanzo.miyazawa@gmail.com

1 Methods

1.1 Knowledge of protein folding

A protein folding theory (3), which is based on a random energy model (REM), indicates that the equilibrium ensemble of amino acid sequences, $\boldsymbol{\sigma} = (\sigma_1, \cdots, \sigma_L)$ where σ_i is the type of amino acid at site i and L is sequence length, should be a canonical ensemble with a Boltzmann factor consisting of the folding free energy, $\Delta G_{ND}(\boldsymbol{\sigma}, T)$ and an effective temperature T_s of natural selection.

$$P(\boldsymbol{\sigma}) \propto P^{\rm mut}(\boldsymbol{\sigma}) \exp(\frac{-\Delta G_{ND}(\boldsymbol{\sigma}, T)}{k_B T_s}) \tag{S1}$$

$$\propto \exp(\frac{-G_N(\boldsymbol{\sigma})}{k_B T_s}) \qquad \text{if } \boldsymbol{f}(\boldsymbol{\sigma}) = \text{constant} \tag{S2}$$

$$\Delta G_{ND}(\boldsymbol{\sigma}, T) \equiv G_N(\boldsymbol{\sigma}) - G_D(\boldsymbol{f}(\boldsymbol{\sigma}), T) \tag{S3}$$

where $p^{\rm mut}(\boldsymbol{f}(\boldsymbol{\sigma}))$ is the probability of a sequence ($\boldsymbol{\sigma}$) randomly occurring in a mutational process and depends only on the amino acid frequencies $\boldsymbol{f}(\boldsymbol{\sigma})$, k_B is the Boltzmann constant, T is a growth temperature, and G_N and G_D are the free energies of the native conformation and denatured state, respectively. Selection temperature T_s quantifies how strong the folding constraints have been during evolution (11), and is specific to the protein structure and function. The free energy G_D of the denatured state does not depend on the amino acid order but the amino acid composition, $\boldsymbol{f}(\boldsymbol{\sigma})$, in a sequence. It is reasonable to assume that mutations independently occur between sites, and therefore the equilibrium frequency of a sequence in the mutational process is equal to the product of the equilibrium frequencies over sites; $P^{\rm mut}(\boldsymbol{\sigma}) = \prod_i p^{\rm mut}(\sigma_i)$, where $p^{\rm mut}(\sigma_i)$ is the equilibrium frequency of σ_i at site i in the mutational process.

The distribution of conformational energies in the denatured state (molten globule state), which consists of conformations as compact as the native conformation. is approximated in the random energy model (REM), particularly the independent interaction model (IIM) (3), to be equal to the energy distribution of randomized sequences, which is then approximated by a Gaussian distribution, in the native conformation. That is, a partition function Z for the denatured state is written as follows with the energy density $n(E)$ of conformations that is approximated by a product of a Gaussian probability density and the total number of conformations whose logarithm is proportional to the chain length.

$$Z = \int \exp(\frac{-E}{k_B T})\, n(E) dE \tag{S4}$$

$$n(E) \approx \exp(\omega L) \mathcal{N}(\bar{E}(\boldsymbol{f}(\boldsymbol{\sigma})), \delta E^2(\boldsymbol{f}(\boldsymbol{\sigma}))) \tag{S5}$$

where ω is the conformational entropy per residue in the compact denatured state, and $\mathcal{N}(\bar{E}(\boldsymbol{f}(\boldsymbol{\sigma})), \delta E^2(\boldsymbol{f}(\boldsymbol{\sigma})))$ is the Gaussian probability density with mean $\bar{E}$ and variance δE^2, which depend only on the amino acid composition of the protein sequence. The free energy of the denatured state is approximated as follows.

$$G_D(\boldsymbol{f}(\boldsymbol{\sigma}), T) \approx \bar{E}(\boldsymbol{f}(\boldsymbol{\sigma})) - \frac{\delta E^2(\boldsymbol{f}(\boldsymbol{\sigma}))}{2 k_B T} - k_B T \omega L \tag{S6}$$

$$= \bar{E}(\boldsymbol{f}(\boldsymbol{\sigma})) - \delta E^2(\boldsymbol{f}(\boldsymbol{\sigma})) \frac{\vartheta(T/T_g)}{k_B T} \tag{S7}$$

$$\vartheta(T/T_g) \equiv \begin{cases} \frac{1}{2}(1 + \frac{T^2}{T_g^2}) & \text{for } T > T_g \\ \frac{T}{T_g} & \text{for } T \le T_g \end{cases} \tag{S8}$$

where $\bar{E}$ and δE^2 are estimated as the mean and variance of interaction energies of randomized sequences in the native conformation. T_g is the glass transition temperature of the protein at which entropy becomes zero (3).

$$-\frac{\partial G_D}{\partial T}|_{T=T_g} = 0 \tag{S9}$$

The conformational entropy per residue ω in the compact denatured state can be represented with T_g.

$$\omega L = \frac{\delta E^2}{2(k_B T_g)^2} \tag{S10}$$

Thus, unless $T_g < T_m$, a protein will be trapped at local minima on a rugged free energy landscape before it can fold into a unique native structure.

1.2 Probability distribution of homologous sequences in sequence space

The probability distribution $P(\boldsymbol{\sigma})$ of sequences, $\boldsymbol{\sigma} \equiv (\sigma_1, \cdots, \sigma_L)$ where $\sigma_i \in$ {amino acids, deletion}, with maximum entropy in sequence space that satisfies a given amino acid frequency at each site and a given pairwise amino acid frequency at each site pair is a Boltzmann distribution (4, 5).

$$P(\boldsymbol{\sigma}) \propto \exp(-\psi_N(\boldsymbol{\sigma})) \tag{S11}$$

$$\psi_N(\boldsymbol{\sigma}) \equiv -(\sum_{i}^{L}(h_i(\sigma_i) + \sum_{j>i} J_{ij}(\sigma_i, \sigma_j))) \tag{S12}$$

where h_i and J_{ij} are one-body and two-body interactions and must satisfy the following constraints.

$$\sum_{\boldsymbol{\sigma}, \sigma_i = a_k} P(\boldsymbol{\sigma}) = P_i(a_k) \tag{S13}$$

$$\sum_{\boldsymbol{\sigma}, \sigma_i = a_k, \sigma_j = a_l} P(\boldsymbol{\sigma}) = P_{ij}(a_k, a_l) \tag{S14}$$

where $P_i(a_k)$ is the frequency of amino acid a_k at site i and $P_{ij}(a_k, a_l)$ is the frequency of amino acid pair, a_k at i and a_l at j; $a_k \in$ {amino acids, deletion}. The pairwise interaction matrix J satisfies $J_{ij}(a_k, a_l) = J_{ji}(a_l, a_k)$ and $J_{ii}(a_k, a_l) = 0$. Interactions h_i and J_{ij} can be well estimated from a multiple sequence alignment (MSA) in the mean field approximation (4, 5), or by maximizing a pseudo-likelihood (6, 7). Here we must notice that $\psi_N(\boldsymbol{\sigma})$ has been estimated under the constraints on amino acid compositions at all sites, and therefore the amino acid composition of a whole sequence must be constant across sequences.

From Eqs. S2 and S11,

$$G_N(\boldsymbol{\sigma}) = k_B T_s[\,\psi_N(\boldsymbol{\sigma}) + \text{function of} \boldsymbol{f}(\boldsymbol{\sigma})\,] \tag{S15}$$

$$G_D(\boldsymbol{f}(\boldsymbol{\sigma}), T) = k_B T_s[\,\psi_D(\boldsymbol{\sigma}) + \text{function of} \boldsymbol{f}(\boldsymbol{\sigma})\,] \tag{S16}$$

$$\Delta G_{ND}(\boldsymbol{\sigma}, T) = k_B T_s\, \Delta\psi_{ND}(\boldsymbol{\sigma}) \tag{S17}$$

$$\Delta\psi_{ND}(\boldsymbol{\sigma}) \equiv \psi_N(\boldsymbol{\sigma}) - \psi_D(\boldsymbol{\sigma}) \tag{S18}$$

$$\psi_D(\boldsymbol{\sigma}) \approx \bar{\psi}(\boldsymbol{f}(\boldsymbol{\sigma})) - \delta\psi^2(\boldsymbol{f}(\boldsymbol{\sigma}))\vartheta(T/T_g)T_s/T \tag{S19}$$

$$\omega = (T_s/T_g)^2\delta\psi^2/(2L) \tag{S20}$$

where $\bar{E} = k_B T_s \bar{\psi}$ and $\delta E^2 = (k_B T_s)^2 \delta\psi^2$. The mean $\bar{\psi}$ and variance $\Delta\psi^2$ are estimated as the mean and variance of ψ_N over randomized sequences in the native structure (3).

1.3 The ensemble average of folding free energy, $\Delta G_{ND}(\boldsymbol{\sigma}, T)$, over sequences

The ensemble average of $\Delta G_{ND}(\boldsymbol{\sigma}, T)$ over sequences with Eq. S1 is

$$\langle \Delta G_{ND}(\boldsymbol{\sigma}, T) \rangle_{\boldsymbol{\sigma}} \tag{S21}$$

$$\equiv \quad [\sum_{\boldsymbol{\sigma}} \Delta G_{ND}(\boldsymbol{\sigma}, T) P^{\mathrm{mut}}(\boldsymbol{\sigma}) \exp(-\frac{\Delta G_{ND}(\boldsymbol{\sigma}, T)}{k_B T_s})\,] \,/\, [\sum_{\boldsymbol{\sigma}} P^{\mathrm{mut}}(\boldsymbol{\sigma}) \exp(-\frac{\Delta G_{ND}(\boldsymbol{\sigma}, T)}{k_B T_s})\,] \tag{S22}$$

$$\approx \quad [\sum_{\boldsymbol{\sigma}\,|\,\boldsymbol{f}(\boldsymbol{\sigma})=\overline{\boldsymbol{f}(\boldsymbol{\sigma}_N)}} G_N(\boldsymbol{\sigma}) \exp(-\frac{G_N(\boldsymbol{\sigma})}{k_B T_s})\,] \,/\, [\sum_{\boldsymbol{\sigma}\,|\,\boldsymbol{f}(\boldsymbol{\sigma})=\overline{\boldsymbol{f}(\boldsymbol{\sigma}_N)}} \exp(-\frac{G_N(\boldsymbol{\sigma})}{k_B T_s})\,] \; - G_D(\overline{\boldsymbol{f}(\boldsymbol{\sigma}_N)}, T) \tag{S23}$$

$$= \quad \langle G_N(\boldsymbol{\sigma}) \rangle_{\boldsymbol{\sigma}} - G_D(\overline{\boldsymbol{f}(\boldsymbol{\sigma}_N)}, T) \tag{S24}$$

where $\boldsymbol{\sigma}_N$ denotes a native sequence, and $\overline{\boldsymbol{f}(\boldsymbol{\sigma}_N)}$ denotes the average of $\boldsymbol{f}(\boldsymbol{\sigma}_N)$ over homologous sequences. In Eq. S23, the sum over all sequences is approximated by the sum over sequences the amino acid composition of which is the same as that of the native sequences. The ensemble average of G_N is also estimated in the Gaussian approximation (3).

$$\langle G_N(\boldsymbol{\sigma}) \rangle_{\boldsymbol{\sigma}} \quad \approx \quad \frac{\int E \exp(-E/(k_B T_s))\, n(E)\, dE}{\int \exp(-E/(k_B T_s))\, n(E)\, dE} \tag{S25}$$

$$= \quad \bar{E}(\overline{\boldsymbol{f}(\boldsymbol{\sigma}_N)}) - \delta E^2(\overline{\boldsymbol{f}(\boldsymbol{\sigma}_N)})/(k_B T_s) \tag{S26}$$

$$\langle \psi_N(\boldsymbol{\sigma}) \rangle_{\boldsymbol{\sigma}} \quad \approx \quad \bar{\psi}(\overline{\boldsymbol{f}(\boldsymbol{\sigma}_N)}) - \delta\psi^2(\overline{\boldsymbol{f}(\boldsymbol{\sigma}_N)}) \tag{S27}$$

The ensemble averages of $\Delta G_{ND}(\boldsymbol{\sigma}, T)$ and $\psi_N(\boldsymbol{\sigma})$ over sequences are observable as the sample averages of $\Delta G_{ND}(\boldsymbol{\sigma}_N, T_s)$ and $\psi_N(\boldsymbol{\sigma}_N)$ over homologous sequences fixed in protein evolution, respectively.

$$\overline{\Delta G_{ND}(\boldsymbol{\sigma}_N, T)} \quad = \quad \langle \Delta G_{ND}(\boldsymbol{\sigma}, T) \rangle_{\boldsymbol{\sigma}} \tag{S28}$$

$$\approx \quad \delta E^2(\overline{\boldsymbol{f}(\boldsymbol{\sigma}_N)})\,[\,\vartheta(T/T_g) T_s/T - 1\,] \tag{S29}$$

$$= \quad k_B T_s \delta\psi^2(\overline{\boldsymbol{f}(\boldsymbol{\sigma}_N)})\,[\,\vartheta(T/T_g) T_s/T - 1\,] \tag{S30}$$

$$\overline{\psi_N(\boldsymbol{\sigma}_N)} \quad \equiv \quad \frac{\sum_{\boldsymbol{\sigma}_N} w_{\boldsymbol{\sigma}_N} \psi_N(\boldsymbol{\sigma}_N)}{\sum_{\boldsymbol{\sigma}_N} w_{\boldsymbol{\sigma}_N}} \tag{S31}$$

$$= \quad \langle \psi_N(\boldsymbol{\sigma}) \rangle_{\boldsymbol{\sigma}} \tag{S32}$$

where the overline denotes sample average with a sample weight $w_{\boldsymbol{\sigma}_N}$ for each homologous sequence, which is used to reduce phylogenetic biases in the set of homologous sequences.

The folding free energy becomes equal to zero at the melting temperature T_m; $\langle \Delta G_{ND}(\boldsymbol{\sigma}_N, T_m) \rangle_{\boldsymbol{\sigma}} = 0$. Thus, the following relationship must be satisfied (3).

$$\vartheta(T_m/T_g)\frac{T_s}{T_m} \quad = \quad \frac{T_s}{2T_m}(1 + \frac{T_m^2}{T_g^2}) = 1 \qquad \text{with } T_s \le T_g \le T_m \tag{S33}$$

1.4 Estimation of $\bar{\psi}(\boldsymbol{f}(\boldsymbol{\sigma}))$ and $\delta\psi^2(\boldsymbol{f}(\boldsymbol{\sigma}))$

The mean $\bar{\psi}(\boldsymbol{f}(\boldsymbol{\sigma}))$ and the variance $\delta\psi^2(\boldsymbol{f}(\boldsymbol{\sigma}))$ in the Gaussian approximation for the distribution of conformational energies at the denatured state are estimated as the mean and variance of ψ_N of random sequences in the native conformation (3).

$$\bar{\psi}(\boldsymbol{f}(\boldsymbol{\sigma})) \quad = \quad -\sum_i [h_i(::) + \sum_{j>i} J_{ij}(::, ::)] \tag{S34}$$

where $h_i(::)$ and $J_{ij}(::, ::)$ are the means of one-body and two-body interactions in random sequences.

$$h_i(::) \quad \equiv \quad \sum_k h_i(a_k) f_{a_k}(\boldsymbol{\sigma}) \tag{S35}$$

$$J_{ij}(::, ::) \quad \equiv \quad \sum_k \sum_l J_{ij}(a_k, a_l) f_{a_k}(\boldsymbol{\sigma}) f_{a_l}(\boldsymbol{\sigma}) \tag{S36}$$

where $f_{a_k}(\boldsymbol{\sigma})$ is the composition of amino acid a_k in the sequence $\boldsymbol{\sigma}$.

$$f_{a_k}(\boldsymbol{\sigma}) = \frac{1}{L}\sum_{i=1}^{L}\delta_{\sigma_i a_k} \tag{S37}$$

where $\delta_{\sigma_i a_k}$ is the Kronecker delta. The variance, $\delta\psi^2(\boldsymbol{f}(\boldsymbol{\sigma}))$, is

$$\delta\psi^2(\boldsymbol{f}(\boldsymbol{\sigma})) = \sum_k f_{a_k}(\boldsymbol{\sigma})\sum_i [\,\delta h_i(a_k)^2 + \sum_{j\neq i}\{\,2\delta h_i(a_k)\delta J_{ij}(a_k,::) \tag{S38}$$

$$+ \sum_{m\neq\{i,j\}}\delta J_{ij}(a_k,::)\delta J_{im}(a_k,::) + \frac{1}{2}\sum_l \delta J_{ij}(a_k,a_l)^2 f_{a_l}(\boldsymbol{\sigma})\,\}\,] \tag{S39}$$

where

$$\delta h_i(a_k) \equiv h_i(a_k) - h_i(::) \tag{S40}$$

$$\delta J_{ij}(a_k,::) \equiv J_{ij}(a_k,::) - J_{ij}(::,::) \tag{S41}$$

$$\delta J_{ij}(a_k,a_l) \equiv J_{ij}(a_k,a_l) - J_{ij}(::,::) \tag{S42}$$

1.5 Estimation of one-body (h) and pairwise (J) interactions

The estimates of h and J (4, 5) are noisy, and J_{ij} may take significant values even for site pairs that are distantly located in the three dimensional structure of protein. Therefore, according to Morcos et al. (11), the estimate of J is modified as follows.

$$\hat{J}_{ij}(a_k,a_l) = J^{\mathrm{g}}_{ij}(a_k,a_l)H(r_{\mathrm{cutoff}} - r_{ij}) \tag{S43}$$

where J^{g} is the statistical estimate of J in a certain gauge, H is the Heaviside step function, and r_{ij} is the distance between the centers of amino acid side chains in protein structure, and r_{cutoff} is a distance threshold for residue pairwise interactions. Maximum interaction ranges employed for pairwise interactions are $r_{\mathrm{cutoff}} \sim 8$ and 15.5Å , which correspond to the first and second interaction shells between residues, respectively. Here it should be noticed that the total interaction $\psi_N(\boldsymbol{\sigma})$ defined by Eq. S12 does not depend on any gauge unless the interaction range for pairwise interactions is limited, but a gauge conversion in which interconversions between h and J occur may change the estimate of $\psi_N(\boldsymbol{\sigma})$ in the present scheme of Eq. S43 in which pairwise interactions are cut off at a certain distance. Thus, a natural gauge must be used before calculating $\hat{J}$.

For example, let us think about the Ising gauge (7), in which h^I and J^I can be calculated from any gauge through the following conversions.

$$J^{\mathrm{I}}_{ij}(a_k,a_l) = J^{\mathrm{g}}_{ij}(a_k,a_l) - J^{\mathrm{g}}_{ij}(a_k,:) - J^{\mathrm{g}}_{ij}(:,a_l) + J^{\mathrm{g}}_{ij}(:,:) \tag{S44}$$

$$h^{\mathrm{I}}(a_k) = h^{\mathrm{g}}_i(a_k) - h^{\mathrm{g}}_i(:) + \sum_{j\neq i}(J^{\mathrm{g}}_{ij}(a_k,:) - J^{\mathrm{g}}_{ij}(:,:)) \tag{S45}$$

where

$$h_i(:) \equiv \frac{1}{q}\sum_{k=1}^{q} h_i(a_k) \tag{S46}$$

$$J_{ij}(:,:) \equiv \frac{1}{q^2}\sum_{k=1}^{q}\sum_{l=1}^{q} J_{ij}(a_k,a_l) \tag{S47}$$

where q is equal to the total number of amino acid types including deletion, that is, $q = 21$. Thus, the gauge conversion of $\hat{J}$ does not affect the total interaction $\psi_N(\boldsymbol{\sigma})$ but the gauge conversion before calculating $\hat{J}$ may significantly change the total interaction.

In the DCA (4, 5), the interaction terms are estimated in the mean field approximation as follows.

$$J^{\mathrm{q}}_{ij}(a_k,a_l) = -(C^{-1})_{ij}(a_k,a_l) \tag{S48}$$

$$J^{\mathrm{q}}_{ij}(a_q,a_l) = J^{\mathrm{q}}_{ij}(a_k,a_q) = J^{\mathrm{q}}_{ij}(a_q,a_q) = 0 \tag{S49}$$

where $i \neq j$ and $1 \leq k, l \leq q-1$, and the covariance matrix C is defined as

$$C_{ij}(a_k, a_l) \equiv P_{ij}(a_k, a_l) - P_i(a_k)P_j(a_l) \tag{S50}$$

Here, one (a_q) of the amino acid types including deletion is used as the reference state; J^{q} denotes the J in this gauge. According to Morcos et al. (4), the probability $P_i(a_k)$ of amino acid a_k at site i and the joint probabilities $P_{ij}(a_k, a_l)$ of amino acids, a_k at site i and a_l at site j, are evaluated by

$$P_i(a_k) = (1-p_c)f_i(a_k) + p_c\frac{1}{q} \tag{S51}$$

$$P_{ij}(a_k, a_l) = (1-p_c)f_{ij}(a_k, a_l) + p_c\frac{1}{q^2} \qquad \text{for} \quad i \neq j \tag{S52}$$

$$P_{ii}(a_k, a_l) = P_i(a_k)\delta_{a_k a_l} \tag{S53}$$

where $0 \leq p_c \leq 1$ is the ratio of pseudocount, and $f_i(a_k)$ is the frequency of amino acid a_k at site i and $f_{ij}(a_k, a_l)$ is the frequency of the site pair, a_k at i and a_l at j, in an alignment; $f_{ii}(a_k, a_l)$ is defined as $f_{ii}(a_k, a_l) = f_i(a_k)\delta_{a_k a_l}$. Then, according to Morcos et al. (4), the one body interactions $h_i(a_k)$ are estimated in the isolated two-state model, that is,

$$P_i(a_k) \propto \exp\left[\, h^{\mathrm{q}}_{ij}(a_k) + J^{\mathrm{q}}_{ij}(a_k, a_l) + h^{\mathrm{q}}_{ji}(a_l) \,\right] \tag{S54}$$

$$h^{\mathrm{q}}_i(a_k) = \frac{1}{L-1}\sum_{j \neq i} h^{\mathrm{q}}_{ij}(a_k) \tag{S55}$$

These h^q and J^q in the q gauge are converted to a new gauge, which is called a simple gauge here,

$$h^{\mathrm{s}}_i(a_k) = h^{\mathrm{q}}_i(a_k) - h^{\mathrm{q}}_i(:) \tag{S56}$$

$$J^{\mathrm{s}}_{ij}(a_k, a_l) = J^{\mathrm{q}}_{ij}(a_k, a_l) - J^{\mathrm{q}}_{ij}(:, :) \tag{S57}$$

In this gauge, the reference state is the average state over amino acids including deletion, instead of a specific amino acid (a_q) in the q gauge. The estimate of J in this gauge is used to calculate $\hat{J}$ in Eq. S43.

2 Materials

2.1 Sequence data

We study the single domains of 8 Pfam (14) families and both the single domains and multi-domains from 3 Pfam families. In Table S1, their Pfam ID for a multiple sequence alignment, and Uniprot ID and PDB ID with the starting- and ending-residue positions of the domains are listed. The full alignments for their families at the Pfam are used to estimate one-body interactions h and pairwise interactions J with the DCA program from "http://dca.rice.edu/portal/dca/home" (4, 5). To estimate the sample ($\overline{\psi_N}$) and ensemble ($\langle\psi_N\rangle_\sigma$) averages of the total interaction, M unique sequences with no deletion are used. In order to reduce phylogenetic biases in the set of homologous sequences, we employ a sample weight (w_{σ_N}) for each sequence, which is equal to the inverse of the number of sequences that are less than 20% different from a given sequence in a given set of homologous sequences. Only representatives of unique sequences with no deletion, which are at least 20% different from each other, are used to calculate the changes of the total interaction ($\Delta\psi_N$) due to single nucleotide nonsynonymous substitutions; the number of the representatives is almost equal to $M_{\rm eff}$ in Table S1.

3 Empirical rules found in the analysis of $\Delta\psi_N$

We have examined the changes of ψ_N due to single nucleotide nonsynonymous substitutions over all sites in the homologous sequences of 14 protein families, and have found the following regression equation.

$$\overline{\Delta\psi_N} \approx \alpha_{\psi_N}\frac{\psi_N-\overline{\psi_N}}{L}+\overline{\overline{\Delta\psi_N}} \qquad \text{with } \alpha_{\psi_N}<0 \tag{S58}$$

with correlation coefficients, $r_{\psi_N} > 0.9$, where L is sequence length, $\overline{\psi_N}$ denotes the average of ψ_N over all homologous sequences, and $\overline{\Delta\psi_N}$ and $\overline{\overline{\Delta\psi_N}}$ denote the average of $\Delta\psi_N$ over all single nucleotide synonymous substitutions at all sites in a protein sequence and its total average over all homologous sequences in a protein family, respectively. In addition, the following relationship for the variance of $\Delta\psi_N$ has been found.

$$\begin{aligned}\mathrm{Var}(\Delta\psi_N) &\approx \text{independent of } \psi_N \text{ and} \\ &\quad \text{constant across homologous sequences in every protein family} &\text{(S59)}\\ &= \text{function of } k_BT_s &\text{(S60)}\end{aligned}$$

Because

$$\mathrm{Var}(\Delta G_N) = \text{function that must not explicitly depend on } k_BT_s \text{ but } G_N \tag{S61}$$

the following important relationship has been derived and used to estimate the relative value of T_s against $T_{s,\rm PDZ}$ of the PDZ family.

$$\begin{aligned}\mathrm{Var}(\Delta G_N) &= (k_BT_s)^2\mathrm{Var}(\Delta\psi_N)\\ &\approx \text{constant} &\text{(S62)}\end{aligned}$$

where $\mathrm{Var}(\Delta G_N)$ and $\mathrm{Var}(\Delta\psi_N)$ are the variances of ΔG_N and $\Delta\psi_N$ over all single nucleotide nonsynonymous substitutions at all sites, respectively. These relationships, Eqs. S58 and S62, are also shown in Figs. S3 and S4 , and the regression coefficients (α_{ψ_N}) and correlation coefficients (r_{ψ_N}) are listed in Tables S2 and S5. With estimated T_s and experimental melting temperature T_m, glass transition temperature T_g and folding free energy ΔG_N have been estimated for each protein family on the basis of the REM. The estimates of T_s and T_g are all within a reasonable range, and the estimated values of ΔG_N agree well with their experimental values for 5 protein families, justifying the estimates of T_s.

Table S1: **Protein families, and structures studied.**

Pfam family	UniProt ID	N [a]	N_{eff} [bc]	M [d]	M_{eff} [ce]	L [f]	PDB ID
HTH_3	RPC1_BP434/7-59	15315(15917)	11691.21	6286	4893.73	53	1R69-A:6-58
Nitroreductase	Q97IT9_CLOAB/4-76	6008(6084)	4912.96	1057	854.71	73	3E10-A/B:4-76
SBP_bac_3 [g]	GLNH_ECOLI/27-244	9874(9972)	7374.96	140	99.70	218	1WDN-A:5-222
SBP_bac_3	GLNH_ECOLI/111-204	9712(9898)	7442.85	829	689.64	94	1WDN-A:89-182
OmpA	PAL_ECOLI/73-167	6035(6070)	4920.44	2207	1761.24	95	1OAP-A:52-146
DnaB	DNAB_ECOLI/31-128	1929(1957)	1284.94	1187	697.30	98	1JWE-A:30-127
LysR_substrate [g]	BENM_ACIAD/90-280	25138(25226)	20707.06	85(1)	67.00	191	2F6G-A/B:90-280
LysR_substrate	BENM_ACIAD/163-265	25032(25164)	21144.74	121(1)	99.27	103	2F6G-A/B:163-265
Methyltransf_5 [g]	RSMH_THEMA/8-292	1942(1953)	1286.67	578(2)	357.97	285	1N2X-A:8-292
Methyltransf_5	RSMH_THEMA/137-216	1877(1911)	1033.35	975(2)	465.53	80	1N2X-A:137-216
SH3_1	SRC_HUMAN:90-137	9716(16621)	3842.47	1191	458.31	48	1FMK-A:87-134
ACBP	ACBP_BOVIN/3-82	2130(2526)	1039.06	161	70.72	80	2ABD-A:2-81
PDZ	PTN13_MOUSE/1358-1438	13814(23726)	4748.76	1255	339.99	81	1GM1-A:16-96
Copper-bind	AZUR_PSEAE:24-148	1136(1169)	841.56	67(1)	45.23	125	5AZU-A/B/C/D:4-128

[a] The number of unique sequences and the total number of sequences in parentheses; the full alignments in the Pfam (14) are used.
[b] The effective number of sequences.
[c] A sample weight (w_{σ_N}) for a given sequence is equal to the inverse of the number of sequences that are less than 20% different from the given sequence.
[d] The number of unique sequences that include no deletion unless specified. The number in parentheses indicates the maximum number of deletions allowed.
[e] The effective number of unique sequences that include no deletion or at most the specified number of deletions.
[f] The number of residues.
[g] These proteins consist of two domains, and other ones are single domains.

Table S2: **Parameter values for $r_{\mathbf{cutoff}} \sim 8$ Å** employed for each protein family, and the averages of the total interactions ($\overline{\overline{\psi_N}}$) over all homologous sequences and of the means and the variances of interaction changes ($\overline{\overline{\Delta\psi_N}}$ and $\overline{\mathrm{Var}(\Delta\psi_N)}$) due to single nucleotide nonsynonymous mutations at all sites over all homologous sequences in each protein family.

Pfam family	L	p_c	n_c [a]	r_{cutoff} (Å)	$\bar{\psi}/L$ [b]	$\delta\psi^2/L$ [b]	$\overline{\overline{\psi_N}}/L$ [b]	$\overline{\overline{\Delta\psi_N}}$ [c]	$\overline{\mathrm{Var}(\Delta\psi_N)}$ [c]	r_{ψ_N} for $\overline{\overline{\Delta\psi_N}}$ [d]	α_{ψ_N}	r_{ψ_N} for $(\mathrm{Var}(\Delta\psi_N))^{1/2}$ [e]	α_{ψ_N}
HTH_3	53	0.175	7.434	8.22	−0.2039	2.8837	−3.0712	4.0412	30.8500	−0.94	−1.3671	−0.23	−0.1741
Nitroreductase	73	0.24	6.411	8.39	−0.1153	2.0825	−2.1975	2.9168	11.0879	−0.94	−1.3915	−0.59	−0.5270
SBP_bac_3	218	0.25	9.230	8.10	−0.1000	2.1624	−2.2618	3.1534	12.2140	−0.98	−1.5267	−0.84	−0.8111
SBP_bac_3	94	0.37	8.000	7.90	−0.1634	1.2495	−1.4054	1.8075	5.6101	−0.96	−1.4191	−0.65	−0.5171
OmpA	95	0.169	8.000	8.20	−0.2457	3.9093	−4.1542	6.0657	55.3105	−0.96	−1.5882	−0.47	−0.4471
DnaB	98	0.235	9.653	8.17	−0.2284	3.9976	−4.2291	6.1006	38.5736	−0.96	−1.4654	−0.52	−0.4385
LysR_substrate	191	0.23	7.843	7.87	−0.2248	1.4450	−1.6712	1.9999	6.7385	−0.97	−1.3646	−0.52	−0.5814
LysR_substrate	103	0.265	8.835	8.25	−0.2240	1.4132	−1.6372	2.0309	7.4763	−0.99	−1.4629	−0.78	−0.6311
Methyltransf_5	285	0.13	7.993	7.78	−0.1462	7.2435	−7.3887	12.2738	127.1400	−0.99	−1.7945	−0.08	−0.0461
Methyltransf_5	80	0.18	6.775	7.85	−0.1763	5.5162	−5.6896	8.7386	61.5293	−0.96	−1.5601	0.06	0.0612
SH3_1	48	0.14	6.417	8.01	−0.1348	3.9109	−4.0434	5.4273	39.8445	−0.94	−1.4457	−0.22	−0.1995
ACBP	80	0.22	9.175	8.24	−0.0525	4.6411	−4.7084	7.8272	55.1762	−0.97	−1.6189	−0.30	−0.1986
PDZ	81	0.205	9.061	8.16	−0.2398	3.1140	−3.3572	4.3897	21.0789	−0.96	−1.5014	−0.43	−0.3293
Copper-bind	125	0.23	9.232	8.26	−0.0838	4.1946	−4.2657	7.2514	51.7793	−0.98	−1.9254	−0.20	−0.1475

[a] The average number of contact residues per site within the cutoff distance; the center of side chain is used to represent a residue.
[b] M unique sequences without deletions are used with a sample weight (w_{σ_N}) for each sequence; w_{σ_N} is equal to the inverse of the number of sequences that are less than 20% different from a given sequence. The M and the effective number M_{eff} of the sequences are listed for each protein family in Table S1.
[c] Representatives of unique sequences without deletions, which are at least 20% different from each other, are used; the number of the representatives used is almost equal to M_{eff}. For HTH_3, 4431 sequences are used; abnormal sequences are removed.
[d] The correlation and regression coefficients of $\overline{\overline{\Delta\psi_N}}$ on ψ_N/L;see Eq. S58.
[e] The correlation and regression coefficients of $(\mathrm{Var}(\Delta\psi_N))^{1/2}$ on ψ_N/L.

Table S3: **Thermodynamic quantities estimated with $r_{\mathbf{cutoff}} \sim 8$ Å .**

Pfam family	r [a]	$k_B\hat{T}_s$ [a] (kcal/mol)	$\hat{T}_s$ (°K)	experimental T_m (°K)	$\hat{T}_g$ (°K)	T [b] (°K)	$\hat{\omega}$ [c] (k_B)	$\langle\Delta G_{ND}\rangle$ [d] (kcal/mol)
HTH_3	-	-	116.3	343.7	155.1	298	0.8107	−2.98
Nitroreductase	-	-	194.0	337.0	214.2	298	0.8537	−2.62
SBP_bac_3	-	-	184.8	336.1	207.0	298	0.8622	−8.14
SBP_bac_3	-	-	272.7	336.1	277.7	298	0.6025	−0.99
OmpA	-	-	86.9	320.0	126.8	298	0.9171	−3.16
DnaB	-	-	104.0	312.8	139.7	298	1.1082	−2.52
LysR_substrate	-	-	248.8	338.0	258.0	298	0.6722	−3.46
LysR_substrate	-	-	236.2	338.0	247.7	298	0.6425	−2.05
Methyltransf_5	-	-	57.3	375.0	107.8	298	1.0220	−39.91
Methyltransf_5	-	-	82.3	375.0	131.7	298	1.0783	−11.14
SH3_1	0.86	0.1583	102.3	344.0	143.8	295	0.9904	−3.68
ACBP	0.82	0.1169	87.0	324.4	127.6	278	1.0774	−6.51
PDZ	0.93	0.2794	140.7	312.9	168.5	298	1.0854	−1.81
Copper-bind	0.83	0.1781	89.8	359.3	135.8	298	0.9171	−11.55

[a] Reflective correlation (r) and regression ($k_B\hat{T}_s$) coefficients for least-squares regression lines of experimental $\Delta\Delta G_{ND}$ on $\Delta\psi_N$ through the origin.
[b] Temperatures are set up for comparison to be equal to the experimental temperatures for ΔG_{ND} or to 298°K if unavailable; see Table S4 for the experimental data.
[c] Conformational entropy per residue, in k_B units, in the denatured molten-globule state; see Eq. S20.
[d] Folding free energy in kcal/mol units; see Eq. S30.

Table S4: **Experimental data used.**

Pfam family	experimental values T_m (°K)	T (°K)	ΔG_{ND} (kcal/mol)	ref. for T_m	ref. for ΔG_{ND} and $\Delta\Delta G_{ND}$
HTH_3	343.7	298	-5.33 ± 0.36	(20)	(22)
Nitroreductase	337.0	-	-	(23)	
SBP_bac_3	336.1	-	-	(24)	
OmpA	320.0	-	-	(25)	
DnaB	312.8	-	-	(26)	
LysR_substrate	338.0	-	-	(27)	
Methyltransf_5	375.0	-	-	(28, 29)	
SH3_1	344.0	295	-3.70	(30)	(31)
ACBP	324.4	278	-8.08 ± 0.08	(32)	(33)
PDZ	312.9	298	-2.90	(34)	(15, 35)
Copper-bind	359.3	298	-12.90 ± 0.36	(36)	(21)

Table S5: **Parameter values for $r_{\mathbf{cutoff}} \sim 15.5$ Å** employed for each protein family, and the averages of the total interactions ($\overline{\overline{\psi_N}}$) over all homologous sequences and of the means and the variances of interaction changes ($\overline{\overline{\Delta\psi_N}}$ and $\overline{\mathrm{Var}(\Delta\psi_N)}$) due to single nucleotide nonsynonymous mutations at all sites over all homologous sequences in each protein family.

Pfam family	L	p_c	n_c [a]	r_{cutoff} (Å)	$\bar{\psi}/L$ [b]	$\delta\psi^2/L$ [b]	$\overline{\psi_N}/L$ [b]	$\overline{\overline{\Delta\psi_N}}$ [c]	$\overline{\mathrm{Var}(\Delta\psi_N)}$ [c]	r_{ψ_N} for $\overline{\overline{\Delta\psi_N}}$ [d]	α_{ψ_N}	r_{ψ_N} for $(\mathrm{Var}(\Delta\psi_N))^{1/2}$ [e]	α_{ψ_N}
HTH_3	53	0.24	32.30	15.46	−0.2591	4.0640	−4.3232	6.3128	48.5075	−0.93	−1.4723	−0.44	−0.2813
Nitroreductase	73	0.32	25.51	15.62	−0.1452	3.3359	−3.4815	5.2466	23.9884	−0.94	−1.5730	−0.68	−0.5961
SBP_bac_3	218	0.35	55.48	15.90	−0.0669	3.4004	−3.4674	5.5888	24.5240	−0.97	−1.6605	−0.84	−0.9034
SBP_bac_3	94	0.455	42.81	15.45	−0.1628	2.3208	−2.4831	3.8780	14.6360	−0.97	−1.6840	−0.77	−0.6742
OmpA	95	0.235	35.58	15.69	−0.2552	5.8175	−6.0757	9.5326	125.0540	−0.95	−1.6945	−0.44	−0.4231
DnaB	98	0.35	46.65	15.57	−0.2351	6.1890	−6.4167	10.3965	67.5994	−0.90	−1.5787	−0.33	−0.3279
LysR_substrate	191	0.33	44.16	15.13	−0.2668	2.3641	−2.6309	3.7028	14.7899	−0.96	−1.5508	−0.53	−0.4839
LysR_substrate	103	0.37	44.06	15.60	−0.2834	2.4271	−2.7111	3.8248	17.9478	−0.99	−1.5685	−0.84	−0.6683
Methyltransf_5	285	0.175	53.52	15.53	−0.1687	12.8982	−13.0658	23.2012	369.5520	−0.98	−1.7992	−0.14	−0.1249
Methyltransf_5	80	0.24	37.02	15.11	−0.1632	9.9944	−10.1576	16.9985	194.4250	−0.91	−1.6482	−0.38	−0.3845
SH3_1	48	0.165	28.46	15.76	−0.1350	7.6161	−7.7523	11.5955	187.9570	−0.92	−1.6770	−0.29	−0.2693
ACBP	80	0.28	36.27	15.34	−0.0235	7.4707	−7.4947	13.1960	102.0870	−0.92	−1.6896	0.12	0.1203
PDZ	81	0.33	40.82	15.77	−0.3022	5.2295	−5.5313	8.0540	62.2153	−0.97	−1.7009	−0.35	−0.2408
Copper-bind	125	0.295	44.34	15.43	−0.0934	8.5012	−8.5928	15.4936	102.3600	−0.97	−1.7939	−0.24	−0.2361

[a] The average number of contact residues per site within the cutoff distance; the center of side chain is used to represent a residue.
[b] M unique sequences without deletions are used with a sample weight (w_{σ_N}) for each sequence; w_{σ_N} is equal to the inverse of the number of sequences that are less than 20% different from a given sequence. The M and the effective number M_{eff} of the sequences are listed for each protein family in Table S1.
[c] Representatives of unique sequences without deletions, which are at least 20% different from each other, are used; the number of the representatives used is almost equal to M_{eff}. For HTH_3, 4461 sequences are used; abnormal sequences are removed.
[d] The correlation and regression coefficients of $\overline{\Delta\psi_N}$ on ψ_N/L;see Eq. S58.
[e] The correlation and regression coefficients of $(\mathrm{Var}(\Delta\psi_N))^{1/2}$ on ψ_N/L.

Table S6: **Thermodynamic quantities estimated with $r_{\mathbf{cutoff}} \sim 15.5$ Å .**

Pfam family	r [a]	$k_B\hat{T}_s$ [a] (kcal/mol)	$\hat{T}_s$ (°K)	experimental T_m (°K)	$\hat{T}_g$ (°K)	T [b] (°K)	$\hat{\omega}$ [c] (k_B)	$\langle\Delta G_{ND}\rangle$ [d] (kcal/mol)
HTH_3	-	-	92.3	343.7	135.4	298	0.9452	−3.73
Nitroreductase	-	-	131.3	337.0	165.8	298	1.0466	−4.30
SBP_bac_3	-	-	129.9	336.1	164.5	298	1.0601	−12.76
SBP_bac_3	-	-	168.1	336.1	194.1	298	0.8705	−3.86
OmpA	-	-	57.5	320.0	100.5	298	0.9516	−3.53
DnaB	-	-	78.2	312.8	118.2	298	1.3542	−3.32
LysR_substrate	-	-	167.2	338.0	193.8	298	0.8803	−8.38
LysR_substrate	-	-	151.8	338.0	181.9	298	0.8453	−4.64
Methyltransf_5	-	-	33.5	375.0	81.0	298	1.0994	−45.10
Methyltransf_5	-	-	46.1	375.0	96.0	298	1.1537	−12.95
SH3_1	0.84	0.0821	46.9	344.0	93.1	295	0.9678	−4.13
ACBP	0.82	0.0689	63.7	324.4	107.0	278	1.3220	−8.51
PDZ	0.94	0.1619	81.5	312.9	121.1	298	1.1852	−2.39
Copper-bind	0.89	0.0997	63.6	359.3	111.9	298	1.3710	−18.42

[a] Reflective correlation (r) and regression ($k_B\hat{T}_s$) coefficients for least-squares regression lines of experimental $\Delta\Delta G_{ND}$ on $\Delta\psi_N$ through the origin.

[b] Temperatures are set up for comparison to be equal to the experimental temperatures for ΔG_{ND} or to 298°K if unavailable; see Table S4 for the experimental data.

[c] Conformational entropy per residue, in k_B units, in the denatured molten-globule state; see Eq. S20.

[d] Folding free energy in kcal/mol units; see Eq. S30.

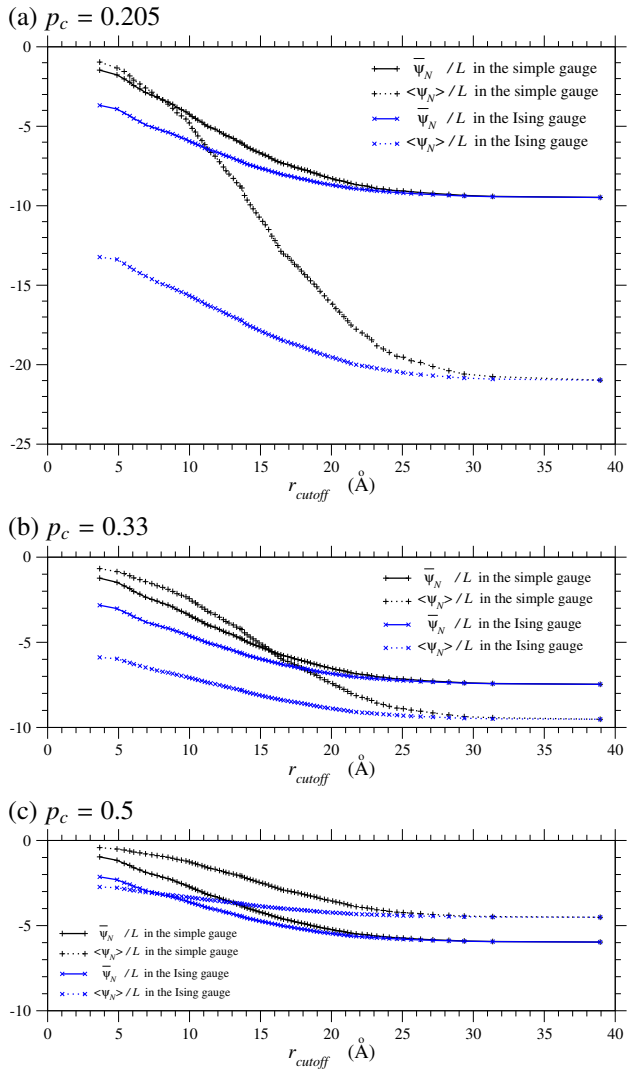


Figure S1: **Dependences of the sample ($\overline{\psi_N}/L$) and ensemble ($\langle\psi_N\rangle_{\boldsymbol{\sigma}}/L$) averages of the total interaction per residue on the cutoff distance for pairwise interactions in the PDZ domain.** The ratios of pseudocount p_c = 0.205 and 0.33 are employed here for the cutoff distance $r_{\mathrm{cutoff}} \sim 8$ and 15.5Å respectively. The solid and dotted lines indicate the sample and ensemble averages, respectively, and black plus and blue cross marks show those for the simple and Ising gauges, respectively.

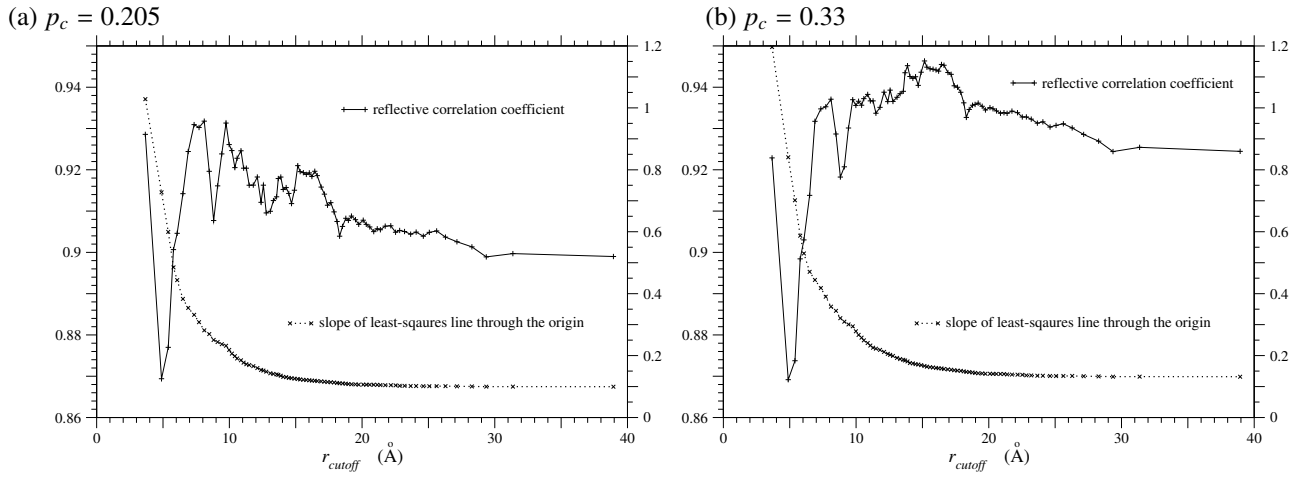


Figure S2: **Dependences of the reflective correlation and regression coefficients between the experimental $\Delta\Delta G_{ND}$ (15) and $\Delta\psi_N$ due to single amino acid substitutions on the cutoff distance for pairwise interactions in the PDZ domain.** The left and right figures are for the ratios of pseudocount, p_c = 0.205 and 0.33, respectively. The solid and dotted lines show the reflective correlation and regression coefficients for the least-squares regression line through the origin, respectively. The sample ($\overline{\psi_N}/L$) and ensemble ($\langle\psi_N\rangle_{\boldsymbol{\sigma}}/L$) averages of the total interaction agree with each other at the cutoff distance $r_{\mathrm{cutoff}} \sim 8$ Å for p_c = 0.205 and $r_{\mathrm{cutoff}} \sim 15.5$ Å for p_c = 0.33, where the reflective correlation coefficients attain to the maximum.

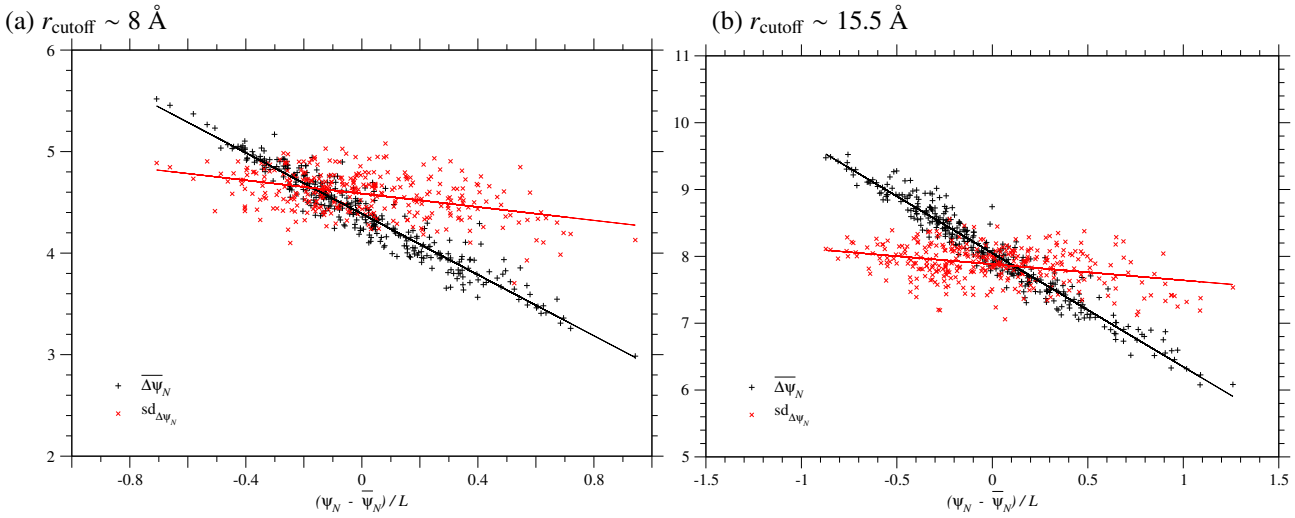


Figure S3: **Correlation between $\Delta\psi_N$ due to single nucleotide nonsynonymous substitutions and ψ_N of homologous sequences in the PDZ domain family.** The left and right figures correspond to the cutoff distance r_{cutoff} ~ 8 and 15.5Å respectively. Each of the black plus or red cross marks corresponds to the mean or the standard deviation of $\Delta\psi_N$ due to all types of single nucleotide nonsynonymous substitutions over all sites in each of the homologous sequences of the PDZ domain family. Only 335 representatives of unique sequences with no deletion, which are at least 20% different from each other, are employed; the number of the representatives is almost equal to M_{eff} in Table S1. The solid lines show the regression lines for the mean and the standard deviation of $\Delta\psi_N$.

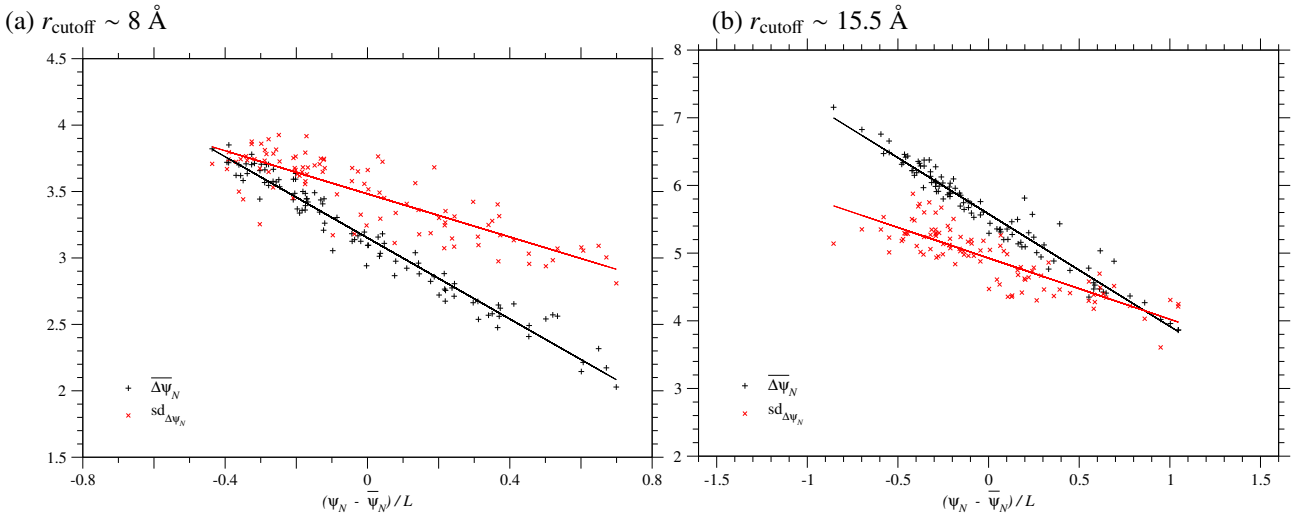


Figure S4: **Correlation between $\Delta\psi_N$ due to single nucleotide nonsynonymous substitutions and ψ_N of homologous sequences in the SBP_bac_3 family of the domain, 1WDN-A:5-222.** The left and right figures correspond to the cutoff distance r_{cutoff} ~ 8 and 15.5Å respectively. Each of the black plus or red cross marks corresponds to the mean or the standard deviation of $\Delta\psi_N$ due to all types of single nucleotide nonsynonymous substitutions over all sites in each of the homologous sequences in the SBP_bac_3 family of the domain, 1WDN-A:5-222. Only 100 representatives of unique sequences with no deletion, which are at least 20% different from each other, are employed; the number of the representatives is almost equal to M_{eff} in Table S1. The solid lines show the regression lines for the mean and the standard deviation of $\Delta\psi_N$.

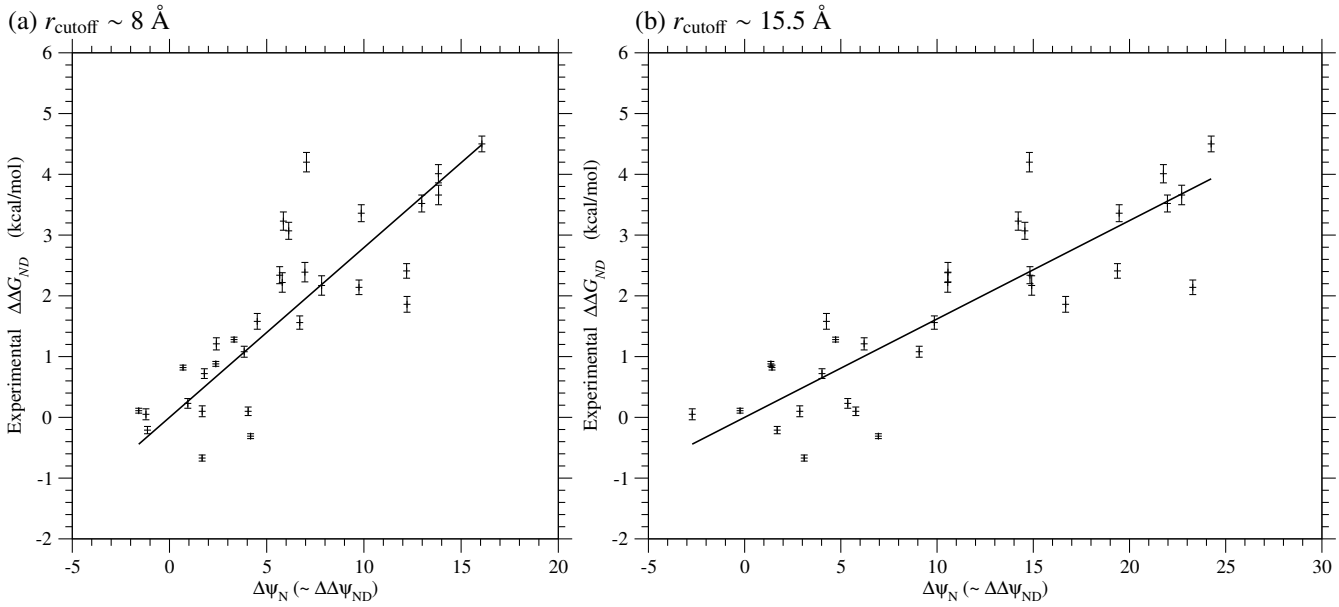


Figure S5: **Regression of the experimental values (15) of folding free energy changes ($\Delta\Delta G_{ND}$) due to single amino acid substitutions on $\Delta\psi_N(\simeq \Delta\Delta\psi_{ND})$ for the same types of substitutions in the PDZ domain.** The left and right figures correspond to the cutoff distance $r_{\mathrm{cutoff}} \sim 8$ and 15.5Å respectively. The solid lines show the least-squares regression lines through the origin with the slopes, 0.279 kcal/mol for $r_{\mathrm{cutoff}} \sim 8$Å and 0.162 kcal/mol for $r_{\mathrm{cutoff}} \sim 15.5$ Å , which are the estimates of $k_B T_s$. The reflective correlation coefficients for them are equal to 0.93 and 0.94, respectively. The free energies are in kcal/mol units.

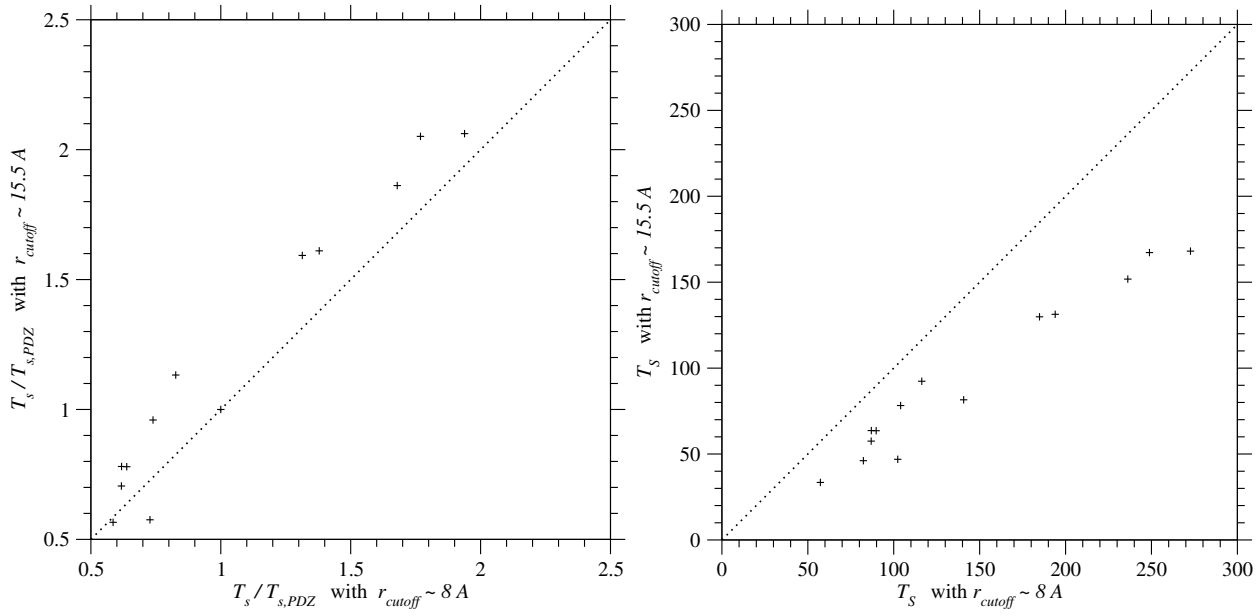


Figure S6: **Comparison of selection temperatures (T_s) estimated with different cutoff distances by the present method.** The abscissa and ordinate correspond to the cases of $r_{\text{cutoff}} \sim 8$ and 15.5Å respectively. The T_s is in °K units.

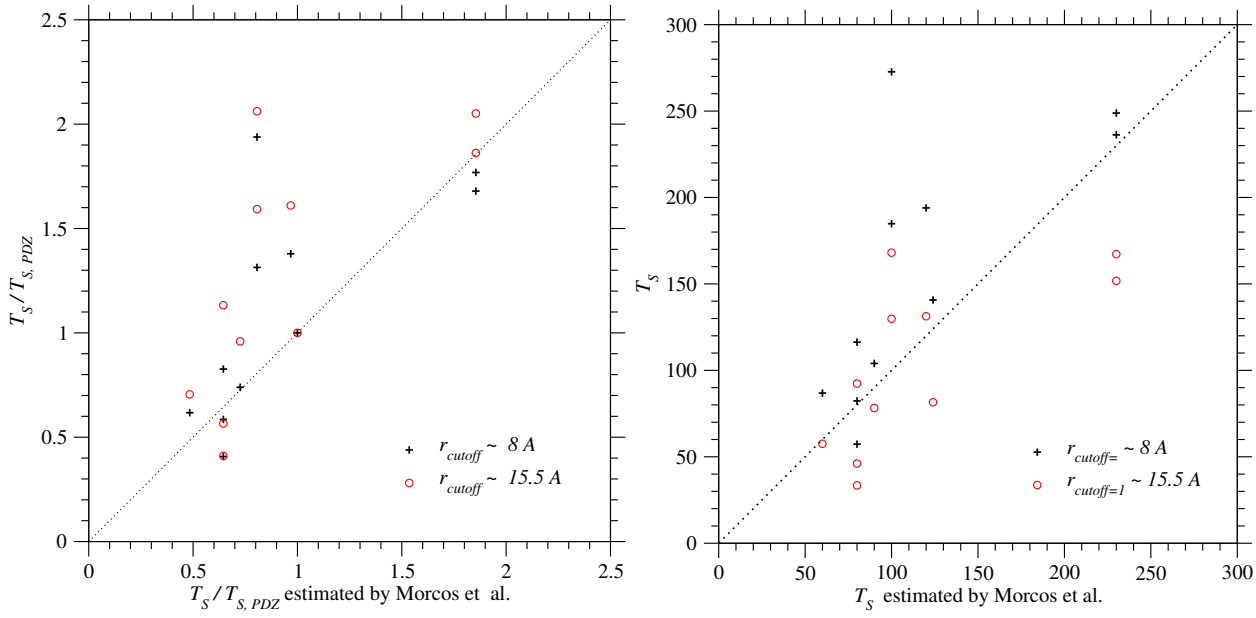


Figure S7: **Selection temperatures (T_s) estimated by the present method are plotted against those estimated by Morcos et al. (11). Plus and open circle marks correspond to the cases of $r_{\mathbf{cutoff}}$ ~ 8 and 15.5Å, respectively.**

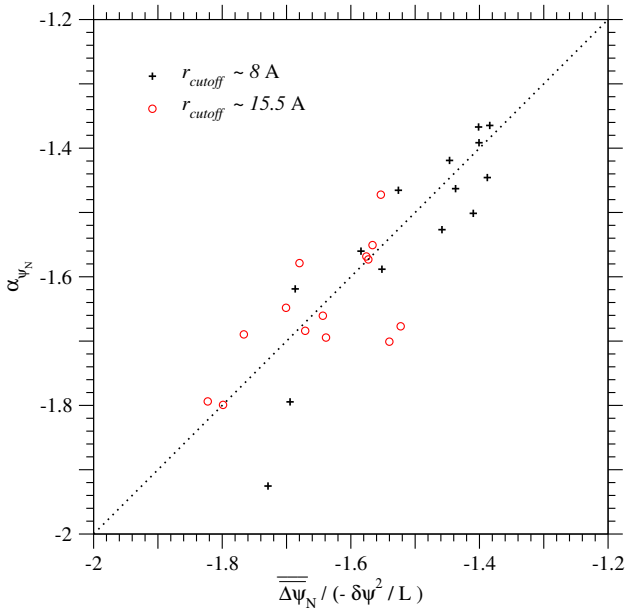


Figure S8: **Comparison of α_{ψ_N}, which is the regression coefficient of $\overline{\Delta\psi_N}$ on ψ_N/L, with $\overline{\overline{\Delta\psi_N}}/(-\delta\psi^2/L)$ for each protein family.** Plus and open circle marks correspond to the cases of $r_{\mathrm{cutoff}} \sim 8$ and 15.5Å, respectively.

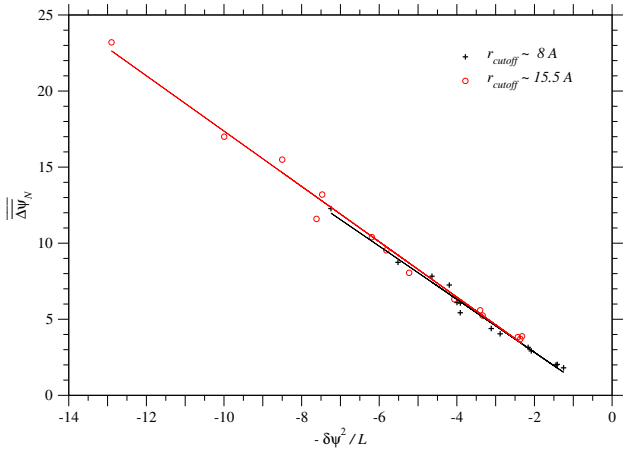


Figure S9: **Dependence of the average of $\overline{\Delta\psi_N}$ due to single nucleotide nonsynonymous substitutions over homologous sequences on $-\delta\psi^2/L$ across protein families.** Plus and open circle marks indicate the values for each protein family in the cases of $r_{\text{cutoff}} \sim 8$ and 15.5Å, respectively. In the case of the cutoff distance 8 Å, the correlation coefficient is equal to 0.99, and the regression line is $\overline{\overline{\Delta\psi_N(\sigma^N_{j\neq i}, \sigma^N_i \to \sigma_i)}} = -1.75(-\delta\psi^2/L) - 0.67$. In the case of $r_{\text{cutoff}} \sim 16$Å, the correlation coefficient is equal to 0.995, and the regression line is $\overline{\overline{\Delta\psi_N(\sigma^N_{j\neq i}, \sigma^N_i \to \sigma_i)}} = -1.82(-\delta\psi^2/L) - 0.81$.

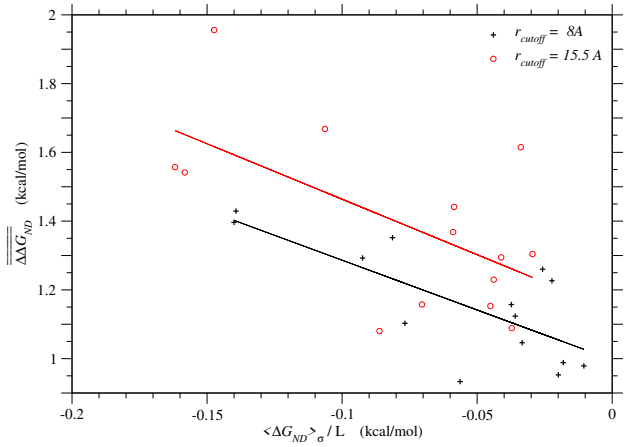


Figure S10: **The sample average of folding free energy change, $\overline{\overline{\Delta\Delta G_{ND}}} = k_B T_s \overline{\overline{\Delta\Delta\psi_{ND}}}$, is plotted against the ensemble average of folding free energy per residue, $\langle\Delta G_{ND}\rangle_{\boldsymbol{\sigma}}/L = k_B T_s \langle\Delta\psi_{ND}\rangle_{\boldsymbol{\sigma}}/L$, for each protein family.** In the case of the cutoff distance 8 Å, the correlation coefficient is $r = -0.74$, and the regression line is $\overline{\Delta\Delta G_{ND}(\sigma^N_{j\neq i}, \sigma^N_i \rightarrow \sigma_i)} = -2.90\langle\Delta G_{ND}\rangle_{\boldsymbol{\sigma}}/L + 1.00$. In the case of $r_{\text{cutoff}} \sim 16$ Å, the correlation coefficient is $r = -0.60$, and the regression line is $\overline{\Delta\Delta G_{ND}(\sigma^N_{j\neq i}, \sigma^N_i \rightarrow \sigma_i)} = -3.23\langle\Delta G_{ND}\rangle_{\boldsymbol{\sigma}}/L + 1.14$. The free energies are in kcal/mol units.

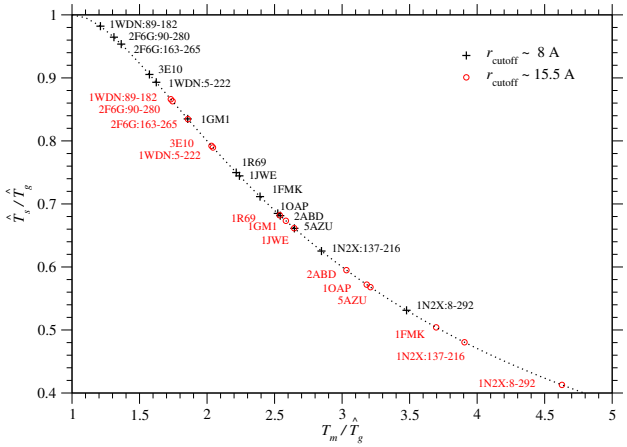


Figure S11: $\hat{T}_s/\hat{T}_g$ **is plotted against** $T_m/\hat{T}_g$ **for each protein domain.** A dotted curve corresponds to Eq. S33, $\hat{T}_s/\hat{T}_g = 2(T_m/\hat{T}_g)/((T_m/\hat{T}_g)^2 + 1)$. Plus and open circle marks indicate the values estimated with $r_{\text{cutoff}} \sim 8$ and 15.5Å , respectively. The T_s and T_g must satisfy $T_s < T_g < T_m$ for proteins to be able to fold into unique native structures.

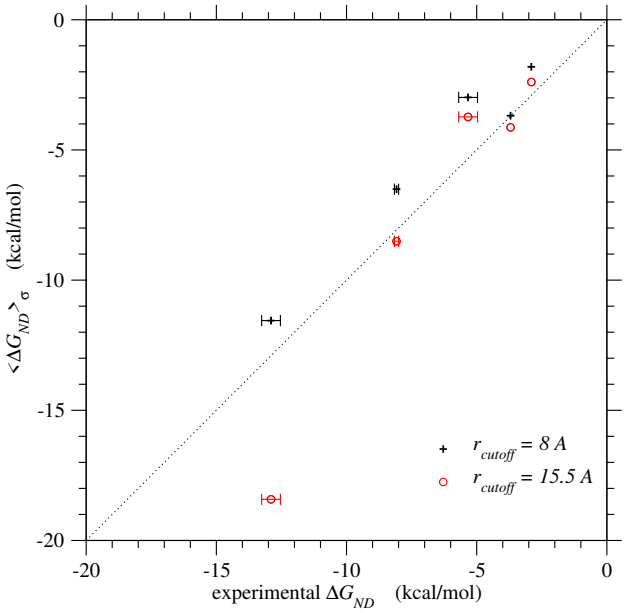


Figure S12: **Folding free energies, $\langle \Delta G_{ND} \rangle_{\sigma}$, predicted by the present method are plotted against their experimental values, $\Delta G_{ND}(\sigma_N)$.** The free energies are in kcal/mol units.